DISCRETE ELEMENT METHOD MODEL OF THE FIRST BREAK WHEAT MILLING PROCESS

by

ABHAY PATWA

B.Tech., Osmania University, 2012

A THESIS

Submitted in partial fulfillment of the requirements for the degree

MASTER OF SCIENCE

Department of Grain Science and Industry
College of Agriculture

KANSAS STATE UNIVERSITY
Manhattan, Kansas

2014

Approved by:

Major Professor
Kingsly Ambrose

Copyright

Abstract

It is a well-known phenomenon that the break-release, particle size and size distribution of wheat milling are functions of machine operational parameters and grain properties. Due to the non-uniformity in characteristics and properties of wheat kernel, the kernel physical and mechanical properties may affect the size reduction process. The discrete element method (DEM) is a numerical modeling technique that can be used to study and understand the effect of physical and mechanical properties of a material on processing. The overall objective of this study is to develop a DEM model of the 1st break wheat milling process.

In this study, different physical and mechanical properties of wheat mill streams were determined for using as the input parameters in DEM model development. The particle size and size distribution (PSD), true, bulk and tapped density, young's modulus, coefficient of static and rolling friction, and coefficient of restitution were measured for wheat kernel, 1st break and flour from hard red winter (HRW), hard red spring (HRS), and soft red winter (SRW) wheat. Overall moisture content was found to have a greater significant effect on the physical properties i.e. density and PSD of the mill streams than material properties i.e. Young's modulus, coefficients of friction and coefficient of restitution.

The DEM model of 1st break wheat milling was developed using both single and multi-sphere approaches. The single sphere approach simulated the size reduction of a spherical cluster of bonded particles with mono-sized particles. The model was simulated for hard red winter (HRW) wheat milling at 16% moisture levels and validated using lab scale milling trials giving a PSD of 437.73 μm with a percent deviation of prediction of 235.37. The deviation of prediction was reduced to 192.29 with a mean PSD of 371.52 μm by conducting sensitivity analysis by modifying the shear modulus and coefficient of restitution values. In the multi-sphere approach, a bonded cluster resembling a wheat kernel in shape and size was used to simulate the milling process. The model predicted a 1st break PSD of 412.65 μm which had a deviation of 185.89 from lab scale and 156.78 from plant scale milling. The model could however satisfactorily predict the variation in PSD from 1st break milling with moisture content with reasonable accuracy. Future capabilities using the model include performing additional sensitivity analysis to understand the effect of other mechanical properties of wheat on the 1st break PSD. It can also be used to improve the 1st break release during wheat milling.

Table of Contents

List of Figures

List of Tables

Acknowledgements

I would like to express my sincere gratitude to Dr. Kingsly Ambrose, my major professor for offering me a graduate research assistantship and for his encouragement and support throughout my graduate study here at Kansas State University by providing valuable guidance and feedback. Under his supervision, I have been able to tremendously develop my research skills. I also acknowledge the Department of Grain Science and Industry for funding my study. I would like to extend my gratitude and appreciation to Dr. Hulya Dogan and Dr. Mark Casada for serving on my committee and providing me with valuable inputs during the advisory committee meetings.

I would like to acknowledge Dr. Susan Sun for allowing the use of the Instron Universal Testing Machine, Dr. Yonghui Li for training me on the use of the Instron, Dr. Yong Sheng Shi for allowing the use of the tablet press, and Dr. Thomas Pearson (formerly with USDA-ARS) for allowing the use of the Casio Exilim High Speed Camera and Prof. Francis Churchill for allowing me to use the milling lab facilities.

I would like to extend my acknowledgments to Dr. Josephine Boac for helping me learn the EDEM software and the EDEM technical support team for helping me with EDEM every time I faced a difficulty.

I also greatly appreciate the help of Shawn Thiele for collection of wheat samples at Hal Ross Mill for experimental validation, Travise Schmeal for fabricating the instruments for one of the research experiments and the Administrative, Clerical and Business office staff in the GSI Department for their help during my graduate study.

I would also like to express special thanks to all my past and present research group members for their support and help and also to my colleagues and friends at K-State for sharing their experiences and encouragement.

I would like to specially thank my friends A. Abhinav Reddy, Pamu Venkata Sarath, Utsav Sharma, and Gaurang Mistry for keeping up with me during the course of my study.

Finally, I would like to thank my Parents for believing in me and being my pillars of strength. Their love, affection and blessings have got me where I am today.

Dedication

To,

My Parents.

Chapter 1 - Introduction

This thesis presents a study on the development of a Discrete Element Method (DEM) model of the 1st break wheat milling process. It involves conducting experiments to determine different properties of wheat mill streams and understand the effect of moisture content on these properties; and the use of these properties as input parameters in the development of the numerical DEM model.

1.1 Problem Statement

Wheat is amongst the largest produced cereal grains around the globe. In 2013-14, 2129 million bushels of wheat were produced in the US alone (USDA ERS, 2014). The primary use of wheat is for human consumption, while a small percentage of the wheat produced is also used towards animal feed, manufacture of alcoholic beverages, etc. In order to be used by the food industry as raw material, wheat needs to be processed into flour. Processing of wheat into flour is a multi-step size reduction process involving operations such as the break-roll system, reduction-roll system, sifting, and purifying systems. Figure 1-1 is a sample flow sheet of a lab scale flour mill comprised of 4 break roll systems and 5 reduction roll systems. After each pass of the grains through a roll, the milled product is screened by sifters of specific sieve opening.

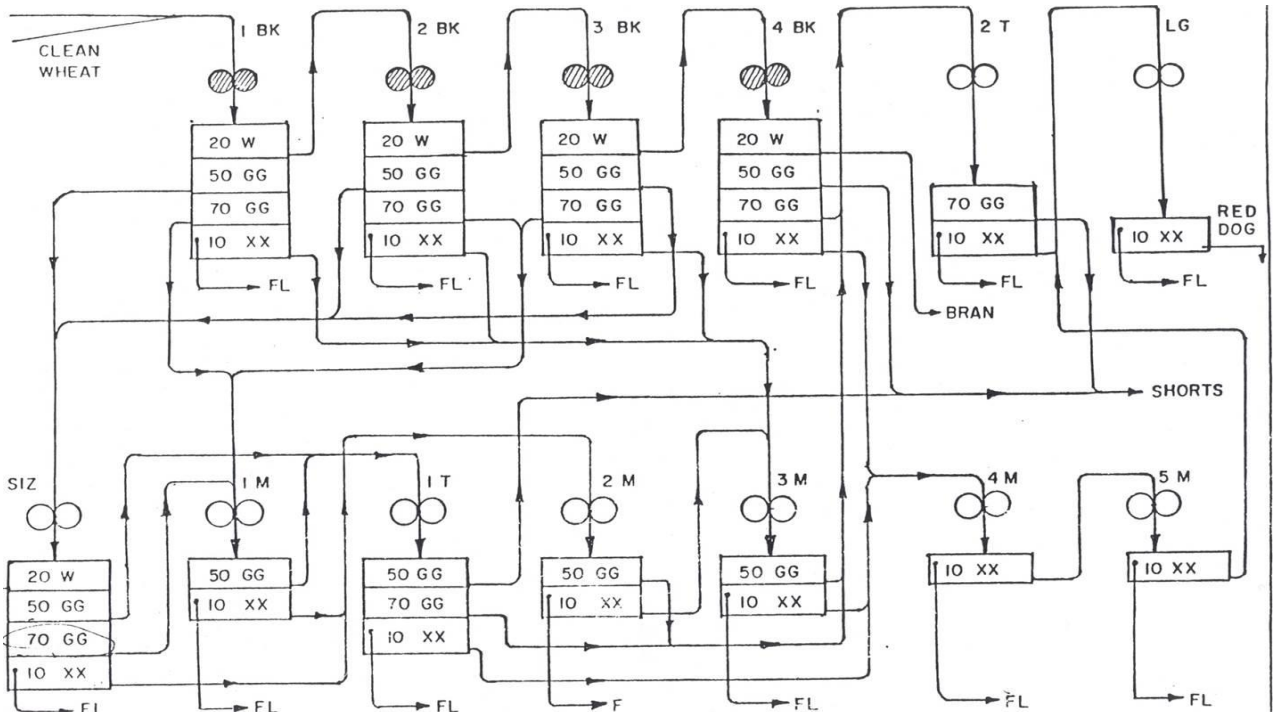

Figure 1-1: Flow-diagram of a lab-scale milling system

The goal of any flour miller is to maintain consistent flour quality (Campbell et al., 2007) while ensuring that the mill is operated at the highest possible efficiency and flour yield. A wheat kernel is made up of nearly 81-84% endosperm, 14-16% bran and 2.5-4% germ (Figure 1-2). Theoretically, the maximum flour extraction rate at which a mill can operate at is 83-84% depending on the bran content. But as the flour extraction rate reaches approximately 80% the quality of flour begins to deteriorate due to visible bran contamination which is highly unfavorable to the consumer.

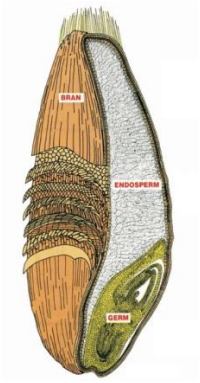

Figure 1-2: Longitudinal section of wheat kernel (source: www.stabroeknews.com)

Bran contamination is one of the factors that affect the flour quality as well as the flour extraction during milling. The quantity of bran present in the flour can be controlled during the break stages, especially 1st break, when the kernel is being opened up in such a way that the bran and germ separate from the endosperm layer (Fang, 1995; Pasikatan, 2000). The subsequent size reduction steps depend to a great extent on the efficiency of the 1st break milling (Niernberger, 1966; Campbell, 2007). The efficiency of the 1st break can be predicted by measuring the break release obtained from this operation (Pasikatan, 2000). However, there are different grain properties and roll variables (Figure 1-3) that affect the efficiency of the 1st break release and eventually the end product quality (Fang et al., 1998). The extent and significance of effect of these variables on the process varies significantly and it is extremely difficult to study simultaneously the effect of all variables especially the physical properties of the ground material (Fang et al., 1998).

Different types of modeling techniques have been used to study the combined and individual effect of most of these variables on wheat milling. Guritno and Haque (1994) developed mathematical relationships, using dimensional analysis, to determine the relationship between the energy and size reduction of wheat in a three roller mill based on the particle size of the milled product. A surface-regression response technique was used by Fang et al., (1998) to determine the significance of the effect of different roll parameters on the energy requirements during 1st break size reduction of wheat. They then used neural network models to predict the properties of the ground material received from the 1st break process. Similarly, Pasikatan et al. (2001) developed two types of linear regression models to predict the energy per unit mass, new specific surface area and specific energy as functions of the wheat class, roll gap, and single kernel properties of wheat. A similar study was conducted by Dziki and Laskowski (2005) to assess the significance of selected factors on the grinding energy of debranned wheat. They developed multiple linear regression models predicting the relationship between these factors and the grinding energy.

Campbell and Webb (2001) were the first to develop a mathematical relationship between the inlet and outlet material particle size and size distribution during the 1st break roller milling operation. They were then able to successfully extend this relationship to predict the effect of several different variables, both grain properties and operational parameters, on the size distribution of the process. Detailed discussions of these modeling techniques are provided in

Chapter 2. These studies were at the bulk level that considered the bulk properties and did not take into account the characteristic non-uniformity of wheat kernels. But for an accurate prediction of the wheat milling process, it is important to consider the wheat kernel mechanical properties which vary from kernel to kernel. Using particle level properties on model development could result in a better prediction model and an understanding of the process as influenced by varying physical and mechanical properties.

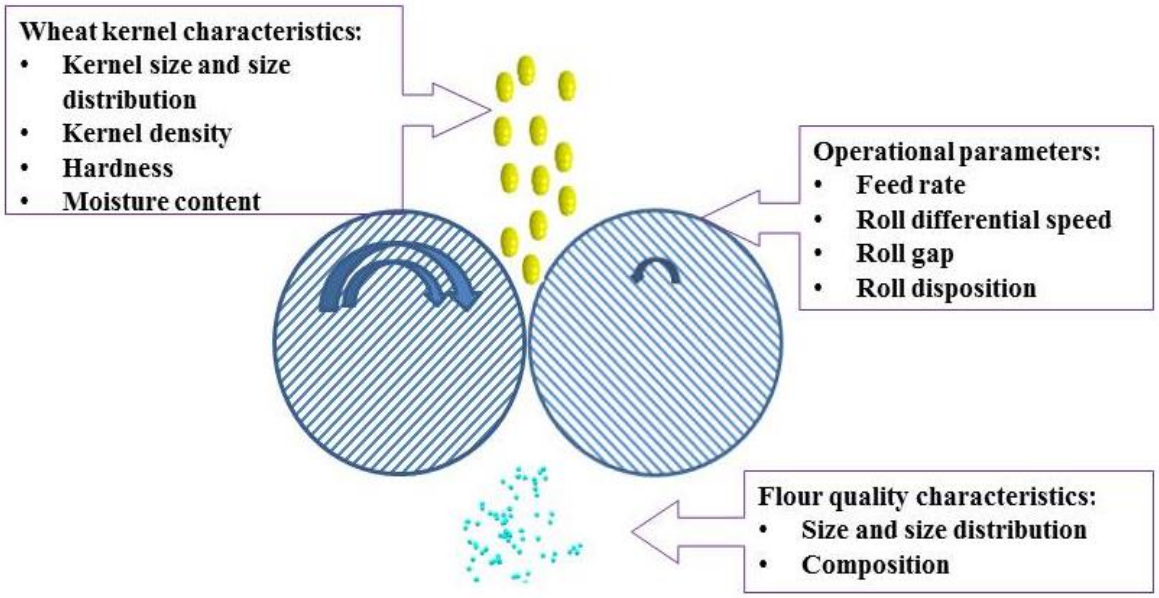

Figure 1-3: Factors affecting the 1st break wheat milling process

1.2 Research Hypothesis and Goals

It is well established that the wheat kernel characteristics and properties differ from kernel to kernel. It is important to understand the behavior of the 1st break milling process from a particle level and with variation in the inherent characteristics of the kernel. The hypothesis of this study is that the mechanical properties of wheat kernels affect the particle size and size distribution of 1st break mill stream.

1.2.1 Research Objectives

To improve the percent flour extraction from wheat, it is important to have an efficient 1st break during milling. In this study, a range of physical and mechanical properties were used as inputs to develop a numerical model of the 1st break size reduction of wheat. The overall objective of this study was to develop a DEM model of the 1st break wheat milling process. The specific objectives of the study were:

1. To determine the effect of moisture content on the physical and material properties of wheat mill streams from three different wheat classes.
2. To develop and validate a DEM model of the 1st break milling of Hard Red Winter (HRW) wheat using a single sphere approach.
3. To develop and validate a multi-sphere DEM model of the 1st break wheat milling with varied bond strength.

1.3 Thesis Outline

The thesis is divided into five chapters excluding this chapter. Chapter 2 covers the review of literature on the factors affecting the wheat milling process, the need to model it, and the different techniques that have been employed for modeling wheat milling. The chapter also includes an introduction to DEM and the working principle. In chapter 3, the techniques used to determine the different physical and mechanical properties of wheat milling streams, i.e. wheat kernels, 1st/2nd break stream and wheat flour, for three different wheat classes and the effect of moisture content on these properties are discussed. The physical and mechanical properties measured were used as input parameters in developing the DEM model. Chapter 4 describes the development of a single sphere DEM model of the 1st break wheat milling process of HRW wheat and the lab scale milling procedures used for validation of the model. Further discussions are provided on the sensitivity analysis of the model. The rationale behind performing sensitivity analysis was to determine the effect of the change in mechanical properties of the wheat kernels on the particle size and size distribution and more importantly to reduce the mean relative percent deviation of the model. In Chapter 5, a multi-sphere DEM model is developed and compared to experimental results. The effect of varying the particle bond strength within the wheat kernel is also described in chapter 5. A detailed discussion is provided on the prediction

behavior of the model with changing property values due to the changing moisture content of the wheat kernels.

1.4 References

Campbell, G. M., & Webb, C. (2001). On predicting roller milling performance Part I: the breakage equation. *Powder Technology, 115*(3), 234-242. doi: 10.1016/s0032-5910(00)00348-x

Campbell, G. M. (2007). Roller milling of wheat. In *Handbook of Powder Technology.* Elsevier B. V.

Dziki, D., & Laskowski, J. (2005). Influence of selected factors on wheat grinding energy requirements. *TEKA. Kom. Mot. Energ. Roln.* 5, 56-64.

Fang, Q. (1995). *Effects of physical properties and wheat and operational parameters of roller mills on size reduction.* Masters, Kansas State University, KS, USA.

Fang, Q., Biby, G., Haque, E., Hanna, M. A., & Spillman, C. K. (1998). Neural network modeling of physical properties of ground wheat. *Cereal Chemistry, 75*(2), 251-253. doi: 10.1094/cchem.1998.75.2.251

Guritno, P., & Haque, E. (1994). Relationship between energy and size reduction of grains using a three-roller mill. *Transactions of the ASAE.* 37(4), 1243-1248.

Niernberger, F. F. (1966). *Roll Diameter and Speed - their Effects on First Break Grinding of Wheat.* Master's, Kansas State University.

Pasikatan, M. C. (2000). *Developement of First-Break Grinding Models and a Near-Infrared (NIR) Reflectance Technique for Estimation of First-Break Grinding Fractions as Bases of a Roll Gap Control Algorithm.* Doctor of Philosophy Dissertation, Kansas State University, KS, USA.

Pasikatan, M. C., Milliken, G. A., Steele, J. L., Haque, E., & Spillman, C. K. (2001). Modeling the energy requirements of first-break grinding. *Transactions of the ASAE.* 44(6), 1737-1744.

Chapter 2 - Wheat Milling and Discrete Element Method: Literature Review

2.1 Wheat Milling

Wheat milling is a gradual size reduction process that involves successive passing of the wheat kernel through a system of break rolls, reduction rolls, sifters and purifiers to produce flour. Essentially a wheat kernel is made up of three parts, the starchy endosperm comprising 81-84% of the kernel, the bran layer, comprising 14-16%, and the germ layer, comprising 2.5-4% of the kernel (Campbell et al., 2007).

The objectives of a flour miller is to ensure efficient separation of the endosperm from the bran layers and germ followed by size reduction of the endosperm into flour with minimal bran contamination and supply the customer with the flour of required consistent quality (Posner & Hibbs, 2005). In order to do so, the quality of the final product largely depends on the performance of the first-break roll since the first-break essentially opens up the wheat kernel and releases the endosperm (Pasikatan, 2000). The efficiency of the first-break roll is determined based on the first break-release which is calculated as the percent mass fractions of ground wheat passing through a sieve of aperture size 1041 μm (Pasikatan, 2000). The break-release in turn depends on the roll variables and the grain properties that affect the percent break release during first-break and the extent to which the endosperm is separated from the bran and germ.

2.2 Factors Affecting the Milling Process

The factors affecting the first break-release and in turn the flour yield can broadly be categorized into the machine operational parameters and the grain properties. The machine operational parameters are the roll configuration settings i.e. the roll gap, speed differential, roll corrugation or the grinding action of the roll, feed rate, and roll diameter (Fang, et al., 1998). The grain properties include mainly the grain hardness and the moisture content. Each of these parameters affects the flour extraction but, it is the interdependency of multiple factors that plays an important role in flour extraction and break-release. Extensive work has been performed in the past by various researchers to study the effect of these factors in wheat milling.

2.2.1 Grain Properties

2.2.1.1 Grain Hardness

Grain hardness is one of the most important grain characteristic in terms of wheat milling (Delwiche, 2000; Posner & Hibbs, 2005). It directly affects the milling behavior of wheat in terms of the tempering requirements, flour particle size and milling yield (Turnbull & Rahman, 2002). In addition, grain hardness determines the end-use of the flour produced. In the U.S., wheat is broadly classified into hard, soft and durum wheat based on the hardness index of the kernels. A large difference exists between the hardness of these wheat varieties (Fang, 1995) which is due to genetic factors apart from the environmental factors and chemical composition of the kernel (Turnbull & Rahman, 2002). Determining the hardness is the first step in wheat milling process, mainly to optimize the roll parameters and the number of rolls to be used. Single kernel characterization system (SKCS), near infrared reflectance (NIR), pearling value, etc are some of the techniques that are used for determining grain hardness. Fang (1995), in a study on the effect of the physical properties of wheat and operational parameters of the roller mills on size reduction, found that kernel hardness to be highly correlated to the characteristics of first-break ground material.

2.2.1.2 Moisture Content

Moisture content of grain kernels is the other parameter that affects the milling process and the end product quality. Prior to milling, stored wheat is tempered to a final moisture content of 14 to 15.5% (wet basis) for soft wheat or 15.5 to 17% (wet basis) for hard wheat (Butcher & Stenvert, 1973; Fang & Campbell, 2003; Fang, 1995). The purpose of addition of moisture to the wheat kernel is to toughen the bran (Fang & Campbell, 2003; Niernberger, 1966; Posner & Hibbs, 2005), making it more compliant and resilient (Dziki et al., 2010). Simultaneously, it also mellows down the endosperm, softening it and enhancing the separation of bran and endosperm reducing the formation of bran powder and yielding cleaner break flour. Studies have also indicated a decrease in power consumption of the break rolls as a result of tempering (Fang & Campbell, 2003). Other advantages of tempering wheat, prior to first-break milling, include easy and accurate sifting of stocks and obtaining a final flour moisture content of 14-15% (Fang & Campbell, 2003; Fang, 1995) and a significant decrease in the ash and protein contents of the

milled streams obtained post first break with increasing moisture content from 14.5 to 17.5% (Hsieh et al., 1980).

2.2.2 Machine Operational Parameters

2.2.2.1 Roll Gap

Roll gap is the opening or clearance between the grinding rolls at the nip (Figure 2-1). The roll gap directly affects the size reduction of kernels and the separation of endosperm and bran. The roll gap is adjusted depending on the desired break-release (Pasikatan, 2000) because the variation in grain properties with wheat class cannot be kept constant (Niernberger, 1966). Therefore a roll gap clearance optimized for a certain hard wheat class may not always correspond to the same opening for a soft wheat class. An empirical equation is also proposed by Kuprits (1965) to determine the extraction as a function of the clearance between the rolls and vice versa. Using this equation, the required roll gap for a given wheat class can easily be calculated provided the miller has information on the first break-release they desire.

$$Ex = me^{-nb} \qquad \textbf{2-1}$$

where, *Ex* is the overall extraction; *b* is the clearance between the rolls; *e* is the base of natural logarithms; *m*, *n* are empirical constants dependent on wheat properties and mill parameters.

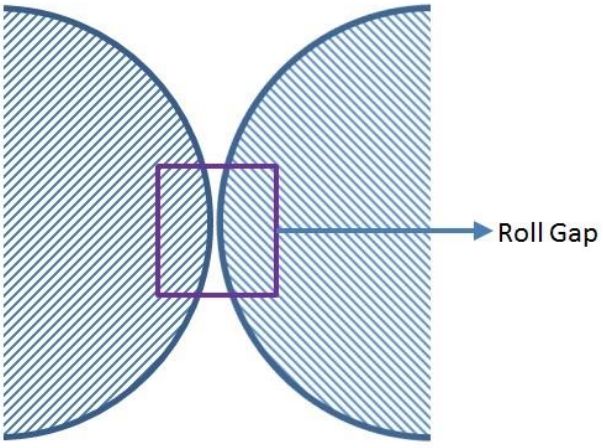

Figure 2-1: Opening between the rolls

Hsieh et al. (1980) studied the effect of three roll gaps, 0.76, 0.89 and 1.02mm, on the first-break grinding of Canadian hard red spring wheat and found that more severe grinding or lower roll gap resulted in a higher break release. The ash content of all streams except overtails also decreased with decreasing roll gap (Hsieh et al., 1980). Guritno and Haque (1994) reported that with decrease in roll gap, the energy utilization and net specific energy consumption increased. They found that reducing roll gap resulted in finer milled products when wheat was milled in a three-roller mill. Similar observations were made by Fang (1995) who reported the effect of three roll gaps (0.66, 0.72 and 0.82mm) on first-break grinding and found it to be positively correlated to the geometric mean particle size and specific energy consumed in a roller mill. In another study, Fang and Campbell (2002) observed that with increase in roll gap (from 0.3 to 0.7 mm) resulted in lesser grain breakage for hard and soft wheat, with greater proportion of larger sized particles and lower proportion of smaller particles.

2.2.2.2 Speed Differential

Speed differential is the ratio of the speed of the fast roll to that of the slow roll. With this difference between the two rolls, a holding action is exerted by the slow roll against the fast roll (Posner & Hibbs, 2005). Compression and shear forces are the two mechanisms that act on kernels during milling wheat. The speed differential helps in creating shearing action and assists the removal of bran with minimum breakage. To have minimum bran contamination in flour, breakage of bran has to be limited within separable limits. Contact time of grain with the rolls depends on the speed differential and influences the compressive and shearing forces to the greater extent. A low speed differential would subject the kernel to less shearing and scraping action and more crushing and flattening action resulting is a low separation of the endosperm and bran (Hsieh et al., 1980). The common practice in flour mills is to operate a speed differential of 2.5:1 in case of break roll systems and 1.25:1 to 1.5:1 in case of the smooth roll reduction system (Posner & Hibbs, 2005).

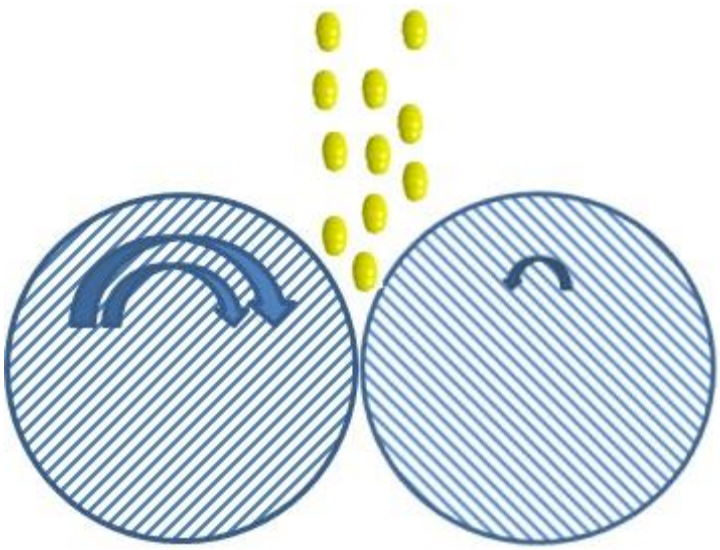

Figure 2-2: Speed differential of the rolls.

(Note: Double arrow = fast roll, single arrow = slow roll)

Hsieh et al. (1980) reported that with the increase in speed differential from 1.5:1 to 3.0:1, the mass percent of all streams except for the overtails increased. The same study reported that the starch damage of first-break flour increased with increasing differential. Tsuge (1985) determined the effect of speed differential, 2.0:1, 2.5:1 and 3.0:1on the characteristics of the middlings extracted from first and second break grindings. The author found that the speed differential of 2.5:1 gave the most satisfactory results of the three differentials tested in terms of the coarseness and ash content of the middlings. The speed differential at first-break had a greater significant effect on the ash content than the first-break roll speed (Tsuge, 1985). Niernberger (1966) also reported that at a constant speed differential of 2.5:1 and at fixed load capacities, the roll speed did not show any significant effect on the particle size and size distribution of the resultant break stream. However, Guritno and Haque (1994) found that, with decrease in the roll speed at a constant differential, the net specific energy consumption and energy utilization increased.

2.2.2.3 Grinding Action of the Rolls

There are four grinding actions depending on the contact of the roll flutings on the slow and fast rolls to the kernels. These are dull-to-dull (D-D), dull-to-sharp (D-S), sharp-to-dull (S-

D), and sharp-to-sharp (S-S) (Figure 2-3). Depending on the stage of milling and the required coarseness of the product, the roll disposition can be changed (Posner & Hibbs, 2005). Kuprits (1965) stated that D-D produced the largest amount of course material with minimum ruptured bran. Similar results were observed by Fang and Campbell (2002). They found that D-D milling disintegrated the fragile endosperm while keeping the bran relatively intact. The kernels in case of D-D grinding actions are subjected to more crushing since the kernels get caught between the back edges of the corrugations. Whereas in case of S-S milling because of the predominant shearing and cutting action (Fang, 1995), the resulting particles are relatively wide and even range of particles sizes since both the endosperm and bran are broken together. The S-D and D-S grinding actions produce a more intermediate product in terms of coarseness when compared to D-D and S-S and are rarely used in wheat milling (Fang, 1995).

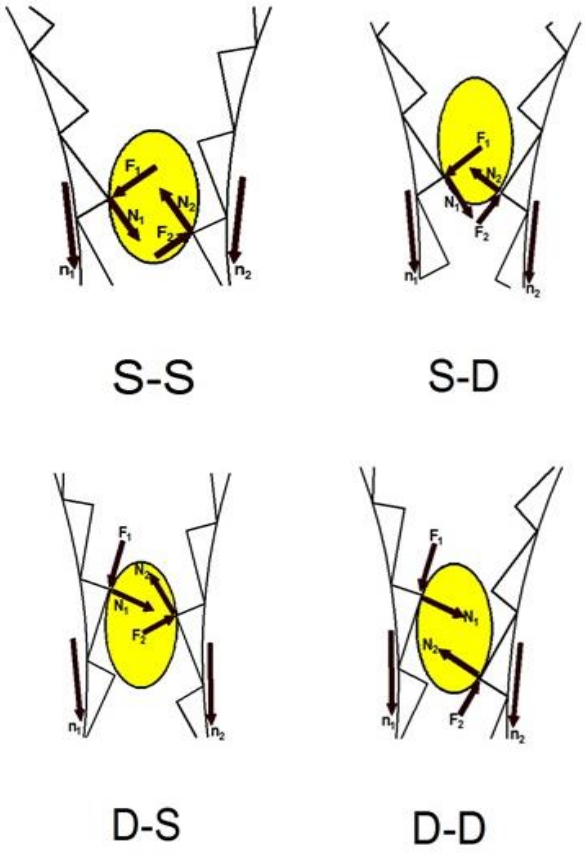

Figure 2-3: Different types of grinding actions (adapted from Campbell et al. 2007)

2.2.2.4 Feed Rate

Feed rate is the amount of material that goes through the grinding zone per unit length of roll per unit time (Pasikatan, 2000). Several authors have reported the theoretical throughput attainable by roller mill of varying diameter (Kuprits, 1965; Niernberger, 1966; Scott, 1951; Speight, 1965). Moog (as cited by Fang (1995)), reported the theoretical maximum to be 7.5 pounds/minute/inch (0.013 kg/min/m). It is also pointed out that actual feed rate used in mills is much lower than this value (Fang, 1995). Niernberger (1966) in his study reported that mills in the U.S., for first-break grinding, operate at 1.0 to 2.5 pounds/minute/inch and European mills operate at capacities ranging from 0.5 to 1.5 pounds/minute/inch while those in Russia and Czechoslovakia operate at 7.0 to 8.11 pounds/minute/inch. Feed rate is dependent on the operating capacity of the roller mill which is determined by the variety of grain, roll gap, roll speed, roll corrugation, and the grinding action (Fang, 1995). It has also been found that the feed rate is the most significant factor affecting the net power consumption but it did not significantly affect the geometric mean particle size, break release or specific grinding energy (Reddy et al., 1998).

2.3 Modeling the Wheat Milling Process

The grain properties and machine variables affect the milling process, 1st break release and the flour yield. Many studies have optimized these variable effects on wheat milling through milling trials and statistical analysis. Computer-based models and simulations have also been used an alternative technique to study these parameters and their effect on the process. Following is a discussion on the various modeling techniques used for studying the effect of different parameters on the wheat milling process.

Fang (1995) used a surface-regression response technique to study the effect of different roll parameters and kernel characteristics on the energy requirements of size reduction of wheat. They successfully developed a first-order regression procedure to predict the power and energy requirements.

$$E_M = 5.927 + 0.0742(H_{SK}) - 22.73(G) + 0.239(M_{SK}) + 0.709(MC) + 2.331(D) - 0.00785(R) \quad \textbf{2-2}$$

$$E_A = -6.023 + 0.0481(H_{SK}) + 10.689(G) - 0.0597(M_{SK}) + 0.564(D) \quad \textbf{2-3}$$

where E_M is the energy per unit mass; E_A is the energy per unit area; H_{SK} is the single kernel hardness; M_{SK} is the single kernel mass; G is the roll gap; MC is the moisture content (% wet basis); R is the fast roll speed (rpm); and D is the speed differential.

In a subsequent study, Fang et al. (1998) developed neural network models to predict the physical properties of ground wheat based on eight input variables. The models were developed to predict the geometric mean diameter, specific surface area increase and the break release. Even though it was claimed that the accuracy of prediction improved substantially when compared to conventional statistical models (Fang et al., 1998), the availability of limited number of data points could have hindered the prediction power of the neural network models. Pasikatan et al. (2001) developed multiple linear regression models to predict the energy per unit mass and energy per unit area consumption during 1st break milling based on the roll gap and single kernel hardness for five different wheat classes. They reported high prediction accuracies of $r^2 = 0.81$ and $r^2 = 0.91$ for the energy per unit mass (Equation 2-4) and energy per unit area (Equation 2-5) respectively.

$$E_M = WCI - 22.439(G) + 0.0641(H_{SK}) + 6.849(S_{SK}) - 0.133(M_{SK}) + 0.499(H_{SD}) - 6.059(S_{SD}) + 0.551(M_{SD}) \quad \textbf{2-4}$$

$$E_A = WCI + 9377(G) + 0.0850(H_{SK}) - 5.219(S_{SK}) + 0.199(M_{SK}) + 0.0669(H_{SD}) + 0.717(S_{SD}) - 0.119(M_{SD}) \quad \textbf{2-5}$$

where WCI is the wheat class-specific intercept; H_{SK} is the single kernel hardness; S_{SK} is the single kernel size or diameter; M_{SK} is the single kernel mass; H_{SD} is the standard deviation of single kernel hardness; S_{SD} is the standard deviation of the single kernel size; M_{SD} is the standard deviation of the single kernel mass; and G is the roll gap.

Pasikatan et al. (2001) further improved these linear regression models to predict the energy per unit mass, new specific surface area and specific energy as functions of the wheat class, roll gap and single kernel properties of wheat. They developed two types of models, the full model by using the roll gap and single kernel size variables, and the reduced model based on milling ratio. For all wheat classes, they reported that the roll gap and single kernel hardness to have consistent significant effects on the response variables.

Campbell and Webb (2001) developed a breakage equation and breakage function to predict the roller milling performance:

$$\rho_2(x) = \int_{D=x}^{D=\alpha} \rho(x, D)\rho_1(D)\, dD \qquad \textbf{2-6}$$

where $\rho_1(D)$ is the particle size distribution of the feed entering the roller mill; $\rho_2(x)$ is the cumulative particle size distribution of the output; and $\rho(x, D)$ is the cumulative breakage function describing the proportion of material smaller than size *x* in the output, originating from an input particle initially of size *D*.

This equation was based on the breakage matrix approach to relate the input and output particle size and size distribution from a roller milling operation (Campbell & Webb, 2001). They further extended the use of this function to determine and predict the effect of different roll parameter and grain properties on the milling performance of the 1st break such as the moisture content (Fang & Campbell, 2003), kernel hardness and shape (Campbell et al., 2007). The model equations incorporating moisture content hardness respectively are given below.

$$\rho_2(x) = \int_0^{m\,max} \int_0^{\infty} B(x, D, m)\, \rho_1(D)\, \rho_2(m)\, dD\, dm \qquad \textbf{2-7}$$

$$\rho_2(x) = \int_{H=0}^{H=\infty} \int_{D=0}^{D=\infty} B(x, D, H)\, \rho_1(D)\, \rho_2(H)\, dD\, dH \qquad \textbf{2-8}$$

where $\rho_1(D)$ is the particle size distribution of the feed entering the roller mill; $\rho_2(x)$ is the cumulative particle size distribution of the output; and; $B(x, D, m/H)$ is the extended breakage function describing the proportion of a material smaller than size *x* produced by a breakage of an inlet particle size *D* and moisture content *m* or hardness *H*.

The above mentioned studies gave successful results and insights on the accuracy of prediction on the performance of the milling process due to the effect of different roll parameters and grain properties. Mateos-Salvador et al. (2011) simplified the breakage equation and developed a double normalized Kumaraswamy breakage function by normalizing the output particle size distribution against the milling ratio raised to a power.

$$P_2(z) \equiv B(x, D) = \alpha(1 - (1 - z^{m_1})^{n_1}) + (1 - \alpha)(1 - (1 - z^{m_2})^{n_2}) \quad \textbf{2-9}$$

where,
$$z = \frac{\chi}{\chi_{max}} \quad \textbf{2-10}$$

and
$$\chi = \frac{x - x_{min}}{\left(G/D\right)^a} \quad \textbf{2-11}$$

where $P_2(z)$ is the cumulative probability distribution function; α is the proportion of breakage that can be described by Type 1 breakage; m_1 and n_1 are parameters corresponding to Type 1 breakage; m_2 and n_2 are parameters corresponding to Type 2 breakage; χ is the normalized particle size; χ_{max} is the maximum measured particle size; *G* is the roll gap; *D* is the average wheat kernel size; *(G/D)* is the milling ratio; and *a* is the collapsing parameter that normalizes data from different milling ratios to fall onto the same curve.

The authors found that these equations to be more versatile and practical for the purpose of design and process integration. Using this normalized Kumaraswamy equation, they were able to take into account the effect of Sharp-to-Sharp and Dull-to-Dull roll dispositions (Mateos-Salvador et al., 2011) and kernel shape and hardness (Campbell et al., 2012) on the milling performance of 1st break roller milling. They were also able to extend this equation to the second break of roller milling (Mateos-Salvador et al., 2013).

All of the studies mentioned above have in one way or the other used different types of statistical models and equations to determine the relationship and significance of different roll parameters and grain properties on the 1st break roller milling process. However, these studies did not take into consideration the physical and mechanical properties of wheat kernels along with their non-uniform characteristics. To develop accurate prediction models for wheat milling, it is very important that the selected numerical method takes into account the highly inconsistent physical and mechanical properties of wheat. In this research work, discrete element modeling (DEM) technique was applied to model the wheat milling process. The DEM technique is reviewed in the following section.

2.4 Discrete Element Method Modeling

The DEM technique was developed by Cundall and Strack (1979) primarily to describe the mechanical behavior of discs and assemblies. Over the past 25 years, the use of DEM has evolved from modeling small scale systems in two dimensions, such as chute flows and small hoppers, to modeling large scale industrial and geophysical systems (Cleary, 2004). Over the past decade, extensive work has been conducted using DEM on granular food material production/handling processes (Boac et al., 2014). The DEM technique has been used to model dragline filling (Coetzee & Els, 2009), screw conveyors (Cleary, 2004), particle separation using vibrating screens (Cleary, 2004), bucket elevators (Boac et al., 2010), flow during discharge (Gonzalez-Montellano et al., 2012), segregation of mixed homogenous material (Ketterhagen et al., 2007).

Size reduction and uniform breakage of particles is a challenge across the solids processing industry. DEM is being used for optimizing these processes in mining, chemical and pharmaceutical industries. Potyondy and Cundall (2004) developed a bonded-particle model (BPM) for rocks that successfully modeled rock breakage. This work paved the way for studies on particle breakage, comminution and size reduction. Metzger and Glasser (2013) incorporated the BPM in the DEM framework to study the breakage of agglomerate particles in ball mill and were successfully able to determine different parameters that significantly affected breakage. With their work they were also able to demonstrate the applicability of DEM in analyzing the breakage in ball mills. Quist (2012) also used the BPM to predict rock breakage in a cone crusher. Both of these studies extensively used BPM in DEM to create non-spherical shaped agglomerates and observe their breakage. Based on the work done by Potyondy and Cundall (2004), this research uses the BPM to model the size reduction of wheat kernels during 1st break milling.

2.4.1 Working Principle of DEM

There are two types of approaches in DEM that can be used depending on the process being modeled. These are the soft-sphere approach and the hard-sphere approach (Boac et al., 2014). The difference between the two is taking into account deformation during collisions. The hard-sphere approach does not take into account deformation of particle during collision while the soft-sphere approach does. Figure 2-4 illustrates the difference between the two types of

approach. In case of soft sphere, the overlap taking place between the particles at the point of contact is an indicator of the deformation that the particle undergoes. The extent of overlap is dependent on the inter-particle contact forces and the resulting motion of the particles is determined making use of contact model (O'Sullivan, 2011). However, the hard sphere approach considers the particle contact as 'shocks' with minimal contact time and is governed by equations of momentum exchange, loss of energy and coefficient of restitution to determine the motion of particle post contact. The hard sphere DEM approach is mainly applicable in case of rapid granular flow simulations since it is computationally cheap. The soft sphere approach is the most commonly used technique in the grain and food processing industries due to its ability to describe the bulk material physics (Boac et al., 2014) which is why we will be using the soft sphere DEM approach as well.

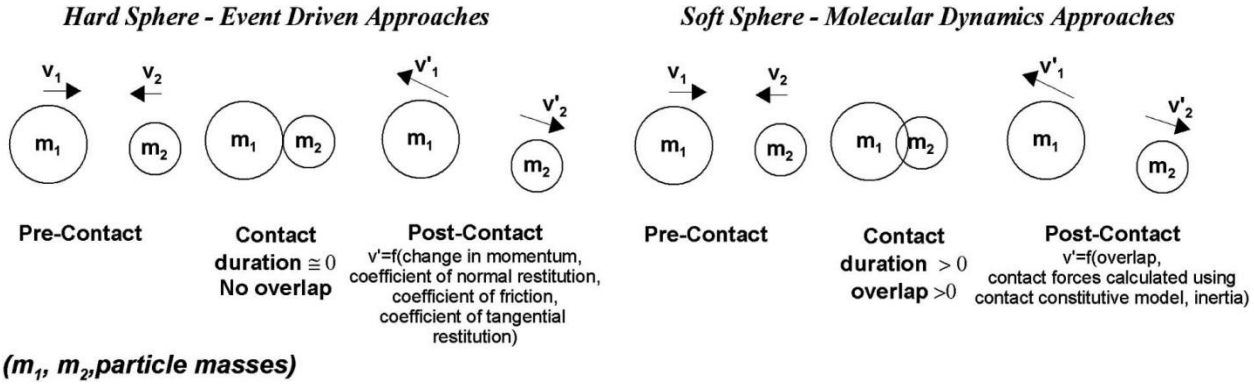

Figure 2-4: Illustration of the differences between hard-sphere and soft-sphere approach in DEM (O'Sullivan, 2011)

DEM is a numerical modeling technique that is based on the principles of Newton's second law of motion and force-displacement laws. It involves monitoring particle interactions at each contact and modeling the particle motion for each particle (Boac et al., 2014). The model generates particles characterized by the physical and mechanical properties of the material under study based on the input parameters given to the model. Depending on the process conditions, DEM models the flow of individual particle and the collisions, contacts, and interactions these particles undergo with other particles and their surrounding environment (Cleary, 2001).

Collisions and contacts cause the forces acting on each particle to change their position, velocity and characteristics. The resultant force is calculated by making use of contact models

based on the force-displacement laws, and the resulting position and velocity data of the particles is calculated using newton's second law of motion. This cycle of calculation of the resulting force, position and velocity of the particles is repeated for each particle for the defined number of time steps which results in simulating the flow of particles in a particle-machine system (Quist, 2012). Therefore, the future of each particle is predicted by the cyclical repetition of an algorithm at every timestep (Gonzalez-Montellano et al., 2012). Figure 2-5 shows the flowchart behind the calculation cycle used in DEM adapted from O'Sullivan (2011).

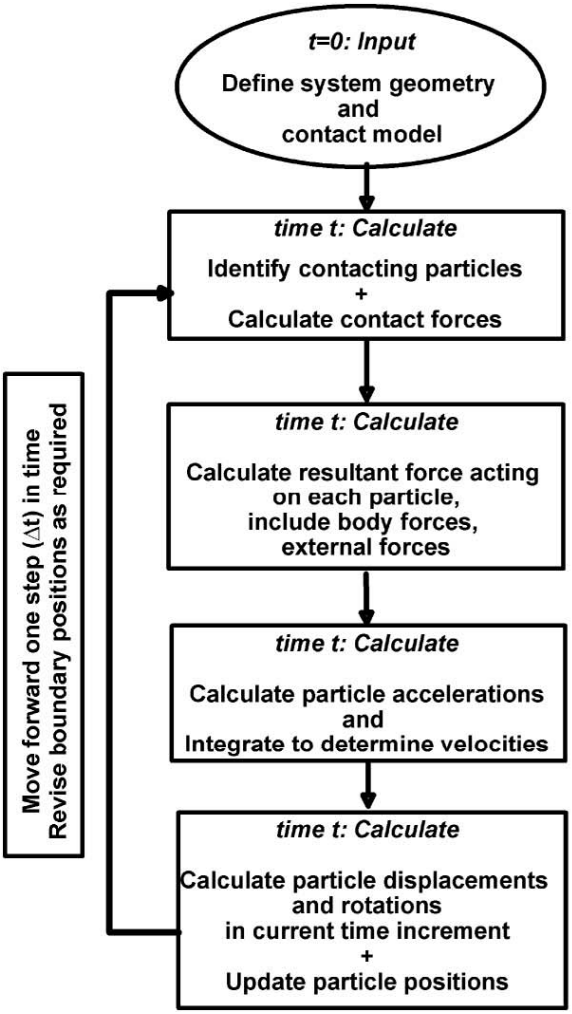

Figure 2-5: DEM calculation cycle flow-sheet (O'Sullivan, 2011)

Contact models are essentially used to determine the force-velocity-displacement during particle contact/collision and model this contact as a mechanical system (Di Renzo & Di Maio, 2004). The simplest mechanical system is a linear spring-dashpot model proposed by Cundall

and Strack (1979) where the spring accounts for the elastic deformation and the dashpot accounts for the viscous dissipation. One of the common variations of the linear spring-dashpot model is the more complex and sound, Hertz-Mindlin and Deresiewicz model. It is based on the Hertz (1882) theory of elastic contacts of spheres in the normal direction and the Mindlin and Deresiewicz (1953) theory that gives the force-deformation relationship of contacting spheres in the tangential direction. However, this model, due to its complexity is considered to be time consuming in case of simulations involving granular flows and is not very popular in application with DEM (Zhu et al., 2007). Depending on the need of the simulating process, various simplified models based on the theories of Hertz and Mindlin and Deresiewicz have also been developed and successfully used in DEM. Walton and Braun (1986) proposed a semi-latched force-displacement model in the normal direction based on the theory of Mindlin and Deresiewicz for cases on constant normal force in the in the tangential direction. Similarly, Thornton and Yin (1991) formulated a more complex model to simulate the tangential force by adopting Hertz theory for determining the normal force. Langston and Tuzun (1994) proposed a more intuitive model by using a direct force-displacement relationship for the tangential force while applying the Hertz theory for the normal force (Zhu et al., 2007). All of the above mentioned models are direct simplifications of the Hertz and Mindlin and Deresiewicz contact theories and have successfully been used to study behavior of granular material (Zhu et al., 2007). In a study by Di Renzo and Di Maio (2004), discussion and comparison of the contact-force models used for simulation of collisions in DEM based granular flow has been done. Although, there are contact models also developed for non-contact forces or inter-particle forces that exist between particles and for particle-fluid interaction forces which can be used within DEM, we have limited the discussion of contact models strictly to the applicability to this research work. Zhu et al. (2007) has done a detailed review of the theoretical development in terms of understanding the microscopic mechanisms and interaction forces in discrete particle simulations of particulate systems. They have discussed the about the different types of contact models that have been developed over the past couple of years and successfully been applied in DEM.

In the DEM working software EDEM (v 2.6, DEM Solutions Ltd., Edinburgh, UK), there are different built-in contact models to suit the phenomena being simulated. These are all listed in the table below. The simplest model referred to as the Hertz-mindlin (no-slip) contact model is

a variant of the spring-dashpot model. It makes use of the elastic theory of Hertz for the normal contacts and *no*-slip solution of tangential contacts obtained from theory proposed by Mindlin and Deresiewicz (Di Renzo & Di Maio, 2004). The other contact models listed in Table 2-1 are variations spring-dashpot model incorporating different aspects of contacts to be applicable to different process simulations. This is also a reason for the increased applicability of DEM in different industries.

Table 2-1: Built-in Contact Models in EDEM Software*

S. No	Contact Model
1.	Hertz-Mindlin (no slip)
2.	Hertz-Mindlin with Bonding
3.	Hertz-Mindlin (no slip) with RVD Rolling Friction
4.	Hertz-mindlin with Archard Wear
5.	Hertz-Mindlin with Heat Conduction
6.	Hertz-Mindlin with JKR Cohesion
7.	Linear Cohesion
8.	Hysteric Spring
9.	Moving Plane
10.	Linear Spring

- Source: EDEM, 2012

To suit this research, we will use the Hertz-Mindlin with bonding contact model. This model enables the calculation of resulting force acting on a particle due to the contacts and interactions it undergoes. According to this, when two particles come in contact, the resultant force due to the overlap, can be calculated as the sum total of the force components in the normal and tangential directions (Gonzalez-Montellano et al., 2012), given by the following equations.

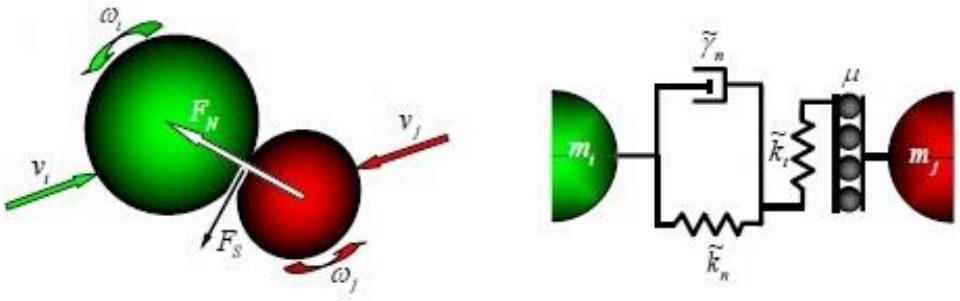

Figure 2-6: Two particle contact and contact model used in EDEM (Metzger, 2011)

$$F = F_n + F_t \quad \textbf{2-12}$$

The normal force F_n, is given as a function of the normal overlap δ_n

$$F_n = \frac{4}{3} E^* \sqrt{R^*} \delta_n^{\frac{3}{2}} \quad \textbf{2-13}$$

Additionally, there is a damping force component F_n^d, given by

$$F_n^d = -2\sqrt{\frac{5}{6}} \beta \sqrt{k_n m^*} V_n^{\overline{rel}} \quad \textbf{2-14}$$

$$m^* = \left(\frac{1}{m_i} + \frac{1}{m_j} \right)^{-1} \quad \textbf{2-15}$$

$$\beta = \frac{\ln e}{\sqrt{\ln^2 e + \pi^2}} \quad \textbf{2-16}$$

$$k_n = 2E^* \sqrt{R^* \delta_n} \quad \textbf{2-17}$$

where, E_i, v_i, R_i and E_j, v_j, R_j denote the Young's modulus, Poissons ratio and radius of each sphere in contact; V_n^{rel} is the normal component of the relative velocity; m^* is the equivalent mass; β is the damping coefficient; k_n is the stiffness; e is the coefficient of restitution; And E^* denotes the equivalent Young's modulus and R^* denotes the equivalent radius, given by

$$\frac{1}{E^*} = \frac{(1 - v_i^2)}{E_i} + \frac{\left(1 - v_j^2\right)}{E_j} \quad \textbf{2-18}$$

$$\frac{1}{R^*} = \frac{1}{R_i} + \frac{1}{R_j} \quad \textbf{2-19}$$

Similarly, the tangential force F_t depends on the tangential overlap δ_t and the tangential stiffness k_t along with the tangential damping coefficient, given by

$$F_t = -k_t \delta_t \quad \textbf{2-20}$$

$$k_t = 8G^* \sqrt{R^* \delta_n} \quad \textbf{2-21}$$

$$F_t^d = -2\sqrt{\frac{5}{6}} \beta \sqrt{k_t m^*} V_t^{\overline{rel}} \quad \textbf{2-22}$$

where G^* is the equivalent shear modulus.

Equations 2-12 to 2-22 were taken from EDEM 2.6 theory reference guide (EDEM 2.6, 2014). The contact model makes use of these equations to determine the force components and resultant forces acting on the particles post collision. As shown in Figure 2-5, after calculations of the forces for the particles at a given time step, the acceleration, displacement and position information of the particles at that time step are determined using newton's second law of motion and the cycle is repeated for the next time step until the end time is reached. Success of this DEM simulation results depends on the accuracy of calculations made by the model which relies on the accuracy of the input parameter values. In this thesis work, the properties required as DEM input values were measured. Using those input parameters, an attempt has been made to predict the first break milling of wheat using DEM.

2.5 References

Boac, J. M., Casada, M. E., Maghirang, R. G., & Harner, J. P., III. (2010). Material and interaction properties of selected grains and oilseeds for modeling discrete particles. *Transactions of the ASABE, 53*(4), 1201-1216.

Boac, J. M., Kingsly, A. R. P., Casada, M. E., Maghirang, R. G., Maier, D. E. (2014). Applications of discrete element method in modeling of grain postharverst operations. *Food Engineering Reviews, 6*(3).

Butcher, J., & Stenvert, N. L. (1973). Conditioning studies on australian wheat. 1. Effect of conditioning on milling behavior. *Journal of the Science of Food and Agriculture, 24*(9), 1055-1066.

Campbell, G. M., Fang, C., & Muhamad, I. I. (2007). On predicting roller milling performance VI - Effect of kernel hardness and shape on the particle size distribution from first break milling of wheat. *Food and Bioproducts Processing, 85*(C1), 7-23.

Campbell, G. M., Sharp, C., Wall, K., Mateos-Salvador, F., Gubatz, S., Huttly, A., & Shewry, P. (2012). Modelling wheat breakage during roller milling using the Double Normalised Kumaraswamy Breakage Function: Effects of kernel shape and hardness. *Journal of Cereal Science, 55*(3), 415-425.

Campbell, G. M., & Webb, C. (2001). On predicting roller milling performance Part I: the breakage equation. *Powder Technology, 115*(3), 234-242.

Cleary, P. W. (2001). Recent advances in DEM modelling of tumbling mills. *Minerals Engineering, 14*(10), 1295-1319.

Cleary, P. W. (2004). Large scale industrial DEM modelling. *Engineering Computations, 21*(2-4), 169-204.

Coetzee, C. J., & Els, D. N. J. (2009). The numerical modelling of excavator bucket filling using DEM. *Journal of Terramechanics, 46*(5), 217-227.

Cundall, P. A., & Strack, O. D. L. (1979). Discrete numerican model for granular assemblies. *Geotechnique, 29*(1), 47-65.

Delwiche, S. R. (2000). Wheat endosperm compressive strength properties as affected by moisture. *Transactions of the ASAE, 43*(2), 365-373.

Di Renzo, A., & Di Maio, F. P. (2004). Comparison of contact-force models for the simulation of collisions in DEM-based granular flow codes. *Chemical Engineering Science, 59*(3), 525-541.

Dziki, D., Laskowski, J., Siastala, M., & Biernacka, B. (2010). Influence of moisture content on the wheat kernel mechanical properties determined on the basis of shear test. *International Agrophysics, 24*(3), 237-242.

EDEM (2012). EDEM 2.4 User guide. DEM Solutions, Edinburgh, UK.

EDEM (2014). EDEM 2.6 Theory reference guide. DEM Solutions, Edinburgh, UK.

Fang, C., & Campbell, G. M. (2003). On predicting roller milling performance V: effect of moisture content on the particle size distribution from first break milling of wheat. *Journal of Cereal Science, 37*(1), 31-41.

Fang, C. Y., & Campbell, G. M. (2002). Effect of roll fluting disposition and roll gap on breakage of wheat kernels during first-break roller milling. *Cereal Chemistry, 79*(4), 518-522.

Fang, Q. (1995). *Effects of physical properties and wheat and operational parameters of roller mills on size reduction.* MS Thesis, Kansas State University.

Fang, Q., Biby, G., Haque, E., Hanna, M. A., & Spillman, C. K. (1998). Neural network modeling of physical properties of ground wheat. *Cereal Chemistry, 75*(2), 251-253.

Fang, Q., Haque, E., Spillman, C. K., Reddy, P. V., & Steele, J. L. (1998). Energy requirements for size reduction of wheat using a roller mill. *Transactions of the ASAE, 41*(6), 1713-1720.

Gonzalez-Montellano, C., Fuentes, J. M., Ayuga-Tellez, E., & Ayuga, F. (2012). Determination of the mechanical properties of maize grains and olives required for use in DEM simulations. *Journal of Food Engineering, 111*(4), 553-562.

Guritno, P., & Haque, E. (1994). Relatioship between energy and size-reduction of grains using a 3-roller mill. *Transactions of the ASAE, 37*(4), 1243-1248.

Hertz, H. (1882). On the contact of elastic body. *Journal of Pure and Applied Mathematics, 92,* 156-171.

Hsieh, F. H., Martin, D. G., Black, H. C., & Tipples, K. H. (1980). Some factors affecting the 1st break grinding of canadian wheat. *Cereal Chemistry, 57*(3), 217-223.

Ketterhagen, W. R., Curtis, J. S., Wassgren, C. R., Kong, A., Narayan, P. J., & Hancock, B. C. (2007). Granular segregation in discharging cylindrical hoppers: A discrete element and experimental study. *Chemical Engineering Science, 62*(22), 6423-6439.

Kuprits, Y. N. (1965). *Technology of Grain Processing and Provender Milling*.

Langston, P. A., & Tuzun, U. (1994). Continuous potential discrete particle simulations of stress and velocity-fields in hoppers - Transition from fluid to granular flow. *Chemical Engineering Science, 49*(8), 1259-1275.

Mateos-Salvador, F., Sadhukhan, J., & Campbell, G. M. (2011). The normalised Kumaraswamy breakage function: A simple model for wheat roller milling. *Powder Technology, 208*(1), 144-157.

Mateos-Salvador, F., Sadhukhan, J., & Campbell, G. M. (2013). Extending the Normalised Kumaraswamy Breakage Function for roller milling of wheat flour stocks to Second Break. *Powder Technology, 237*, 107-116.

Metzger, M. J. (2011). *Numerical and experimental analysis of breakage in a mill using the attainable region approach*. Doctor of Philosophy Dissertation, Rutgers, The State University of New Jersey, NJ, USA.

Metzger, M. J., & Glasser, B. J. (2013). Simulation of the breakage of bonded agglomerates in a ball mill. *Powder Technology, 237*, 286-302.

Mindlin, R. D., & Deresiewicz, H. (1953). Elastic spheres in contact under varying oblique forces. *Journal of Applied Mechanics-Transactions of the ASME, 20*(3), 327-344.

Niernberger, F. F. (1966). *Roll Diameter and Speed - their Effects on First Break Grinding of Wheat.* Master's, Kansas State University.

O'Sullivan, C. (2011). Particle-Based Discrete Element Modeling: Geomechanics Perspective. *International Journal of Geomechanics, 11*(6), 449-464.

Pasikatan, M. C. (2000). *Developement of First-Break Grinding Models and a Near-Infrared (NIR) Reflectance Technique for Estimation of First-Break Grinding Fractions as Bases of a Roll Gap Control Algorithm.* Doctor of Philosophy Dissertation, Kansas State University, KS, USA.

Pasikatan, M. C., Milliken, G. A., Steele, J. L., Haque, E., & Spillman, C. K. (2001). Modeling the energy requirements of first-break grinding. *Transactions of the ASAE, 44*(6), 1737-1744.

Pasikatan, M. C., Milliken, G. A., Steele, J. L., Spillman, C. K., & Haque, E. (2001). Modeling the size properties of first-break ground wheat. *Transactions of the ASAE, 44*(6), 1727-1735.

Posner, E. S., & Hibbs, A. N. (2005). *Wheat flour milling*, second edition. St. Paul, Minn.: AACC International.

Potyondy, D. O., & Cundall, P. A. (2004). A bonded-particle model for rock. *International Journal of Rock Mechanics and Mining Sciences, 41*(8), 1329-1364.

Quist, J. (2012). *Cone crusher modelling and simulation- Developement of a virtual rock crushing environment based on the discrete element method with industrial scale experiments for validation.* Unpublished MS Thesis, Chalmers University of Technology, Goteborg, Sweden.

Reddy, P. V., Fang, Q., Haque, E., Spillman, C. K., & Steele, J. L. (1998). Energy requirements for size reduction of wheat in first break milling. *Bulletin, Association of Operative Millers*(April), 7065-7070.

Scott, J. H. (1951). *Flour milling processess* (2nd ed ed.): Chapman and Hall Ltd. .

Speight, J. (1965). Is the roller mill capable of greater effort? *Milling, 142*(10).

Thornton, C., & Yin, K. K. (1991). Impact of elastic sphere with and without adhesion. *Powder Technology, 65*(1-3), 153-166.

Tsuge, N. (1985). *The effects of the first break roller milling differentals and speeds.* Master of Science Thesis, Kansas State University.

Turnbull, K. M., & Rahman, S. (2002). Endosperm texture in wheat. *Journal of Cereal Science, 36*(3), 327-337.

Walton, O. R., & Braun, R. L. (1986). Stress calculations for assemblies of inelastic sphere in uniform shear. *Acta Mechanica, 63*(1-4), 73-86.

Zhu, H. P., Zhou, Z. Y., Yang, R. Y., & Yu, A. B. (2007). Discrete particle simulation of particulate systems: Theoretical developments. *Chemical Engineering Science, 62*(13), 3378-3396.

Chapter 3 - Determination of Physical and Material Properties of Wheat Mill Stream for Discrete Element Method Modeling

The results have been published and presented at conferences, with the citations below.

Journal publication:

Patwa, A., Ambrose, K., Dogan, H. and Casada, M. E. 2014. Wheat mill stream properties for discrete element method modeling. *Transactions of the ASABE,* 57(3): 891-899.

Conference presentation:

Patwa, A.**,** and Ambrose, K**.** 2013. Wheat mill stream properties for discrete element method modeling. Paper No. 1587727. ASABE, St. Joseph, MI.

3.1 Wheat Milling and the Factors Affecting the Milling Process

Wheat milling is a gradual size reduction process that involves the passing of wheat kernels through a series of break rolls, reduction rolls, sifters, and purifiers. The objective of the milling process is to separate the endosperm from the bran layer and gradually reduce the size of endosperm into flour without the presence of bran in the flour (Posner and Hibbs, 2005). As per the U.S. Code of Federal Regulations (CFR, 2013), for classifying the end product of the milling process as flour, "not less than 98 percent of the flour passes through a cloth having openings not larger than those of woven wire cloth designated 212 µm (No. 70)". Therefore in order to get the highest quality flour at maximum yield, it is necessary to ensure that the 1st operation of milling i.e. the 1st break roller milling operation is performed to its objective. The purpose of 1st break milling is to open up the wheat kernel separating the endosperm from the bran and germ keeping the bran intact without shattering it into smaller particles. However, the efficiency of separation of the endosperm from the bran and germ layers depends on a large number of operational variables and grain properties. The operational variables include the roll gap, speed differential of the rolls, roll disposition, feed rate, etc. The grain properties can be divided into primary and secondary properties. The primary properties include the kernel hardness and moisture content and secondary properties include the particle size and size distribution, bulk density and other strength properties of kernels. A detailed discussion and the effect of these parameters on the 1st break milling efficiency have been discussed in chapter 2.

With the overall objective to develop a DEM model of the 1st break wheat milling process, different physical and mechanical properties of the wheat kernels and break stream are required as input parameters for the model.

3.2 Sample Preparation

Samples of three different classes of wheat, HRW, HRS and SRW wheat were procured from commercial flour manufacturers. These three wheat classes were selected for their distinct and different hardness characteristics. The mill streams studied were the wheat kernel, 1st/2nd roll break stream and wheat flour. Wheat milling involves separation of flour and other streams (such as bran and germ based on size and flour content) once the wheat kernels pass through roller mill. But, most of the flour manufacturers process wheat kernels through 1st and 2nd roller mills (breaks) continuously for efficient flour separation without going through the separation of components after the 1st roller mill (1st break). So, in this study, break stream samples that passed through the 1st and 2nd roller mills (without any intermittent separations) were used for property analyses. The standard roll parameters used for the break milling wheat were: speed differential = 2.5:1, roll disposition = dull-to-dull, roll gap =0.05mm for 1st break and 0.025mm for 2nd break. The moisture content of all samples was determined using the AOAC standard procedure 925.10 (AOAC, 2000) of drying 2-3 g of the sample in a hot air oven for 60 min at 130°C. Each of the samples was conditioned to 12%, 14% and 16% moisture content (wet basis). Proper moisture adjustments for conditioning samples were calculated based on sample dry matter contents (Kingsly et al., 2009). Proximate analysis and starch content determination was performed on the samples by an external lab to determine the chemical composition of break stream and flour. The methods used for analysis included AOAC 934.10 for moisture, AOAC 984.13 for crude protein, AOAC 920.39 for crude fat, AOAC 978.10 for crude fiber, AOAC 942.05 for ash content and AACC 76-13.01 for starch content.

3.3 Physical and Material Properties

3.3.1 Single Kernel Characterization System

A Perten wheat hardness instrument (Model SKCS 4100, Hagersten, Sweden) was used to determine single kernel characteristics. A 12-16g sample was cleaned of foreign material and used for analysis. The instrument analyses 300 kernels individually for diameter, weight, hardness, and moisture content. The measured diameter was reported as the average kernel size.

3.3.2 Particle Size and Size Distribution

A Tyler-Rotap sieve shaker (Model RX-29, Tyler Inc., OH, USA) was used to measure the particle size and particle size distribution of the wheat break stream and flour samples based on ASABE standard S319.4 (ASABE, 2008). 100 g of the sample was placed on the topmost sieve of a set of 14 sieves whose weights were already recorded and sieved for 10 minutes until. The mass of sample retained on each sieve was recorded and the particle size was reported in terms of the geometric mean diameter (d_{gw}) and geometric standard deviation (S_{gw}) using Equations 3-1 & 3-2.

$$d_{gw} = \log^{-1}\left[\frac{\sum_{i=1}^{n}(W_i \log d_i')}{\sum_{i=1}^{n} W_i}\right] \quad \textbf{3-1}$$

$$S_{gw} \approx \frac{1}{2} d_{gw}\left[\log^{-1} S_{log} - \left(\log^{-1} S_{log}\right)^{-1}\right] \quad \textbf{3-2}$$

where d_{gw} is the geometric mean diameter of particles by mass (mm), S_{log} is the geometric standard deviation of log-normal distribution by mass, S_{gw} is the geometric standard deviation of particle diameter by mass (mm), W_i is the mass on the i^{th} sieve (g), n is the number of sieves, d_i is the nominal sieve aperture size of the i^{th} sieve (mm).

For measuring the particle size of wheat flour, a laser diffraction technique (Horiba LA-910, Horiba, Ltd., Kyoto, Japan) was used. Laser diffraction is a volume based wet technique that involves diluting the sample by adding approximately 2g of the sample to 20 ml of distilled water in a centrifuge tube and shaking it thoroughly until the sample dissolves. The diluted sample was poured into the reservoir tank of the instrument which was filled with distilled water.

A set of agitating blades at 400rpm further mixed the flour samples in the water to allow uniform dispersion of the particles in the dispersant. Post agitation and ultrasonic vibrations (39 kHz), light from a He-Ne laser and tungsten lamp is passed through solution and based on the angle of diffraction of the light scattered by the particles, the system uses optical models and mathematical procedures to calculate the particle size of the sample (Horiba LA-910 user guide, 2008).

3.3.3 Bulk Density

A Winchester cup arrangement (Seedburo Equipment Co., Des Plaines, IL, USA) was used to estimate the bulk density of the wheat kernels and mill streams. The samples were made to fall from a hopper into a cup from a height of 10 cm. The cup was allowed to fill completely with the same until excess of it began to overflow. The excess sample was removed by making zig-zag motion with a scrapper. The bulk density was calculated from the weight and volume of the samples.

3.3.4 Tapped Density

Tapped density or compacted bulk density is the ratio of mass to volume of the sample after it has been tapped for a fixed number of times. The Autotap density analyzer (Quantachrome Instruments, FL, USA) was used to measure the tapped density. A cylinder of known volume was filled with each sample and the cylinder was then tapped 750 times (260 taps per minute). The tapped density was calculated from the tapped volume and weight of the samples.

3.3.5 True Density

True density of the mill stream samples was measured using a gas pycnometer (AccuPyyc II, 1340 Micromeritics, GA, USA). Helium gas was used to fill the chamber containing the sample to determine the volume occupied by the particles. The density was calculated from the weight and volume of the solid particles.

3.3.6 Young's Modulus

Young's modulus is the ratio of the stress produced in a body to the applied strain. Young's modulus and yield stress are important material properties that provide information

about the particle deformation behavior (Yap et al., 2008). A universal testing machine (UTM) (Instron 4465, MA, USA) was used to measure the Young's modulus of the wheat mill streams. A cylindrical die, 40 mm in diameter and a close fitting punch were fabricated for this purpose. The die was filled with the sample and compressive forces upto 5kN was applied. The UTM recorded the applied force and displacement produced in the material. Using the resulting strain produced, the Young's modulus was calculated using Equation 3-3 given below. Three replicates were performed for the measurement of Young's modulus of each sample.

$$E = \left(\frac{F/A}{\Delta L/L} \right) \qquad \textbf{3-3}$$

where E is the Young's modulus (MPa), F is the force (kN), A is the area (m^2), L is the length (m) and ΔL is the change in length (m)

3.3.7 Coefficient of Static Friction

The static friction coefficient (μs) between the particle and wall, (a steel plate 30cm x 35cm), was measured using a laboratory device comprised of an open bottom container, test weight, and a pulley system. A known weight of sample filled the open bottom container connected by the string-pulley system to a hanging cup. Weights were placed in the cup in small increments and the end point was determined when the container with sample moved for a corresponding increase in weight. The coefficient of static friction was calculated as the ratio of the weight required to move the sample to the weight of sample.

3.3.8 Coefficient of Rolling Friction

An arrangement similar to that described by Garnayak et al. (2008) was used to measure the coefficient of rolling friction. The sample was poured onto a horizontal steel plate (30cm x 35cm) so that it formed a cone. Using an attached manually driven screw, the inclination of the platform was slowly increased until the sample began to roll down (Jayas and Cenkowski, 2007). The angle of inclination (θ) at this point was determined using the height of the platform from the base and the base length. The coefficient of rolling friction (μ_r) was calculated as the tangent of the angle of inclination.

3.3.9 Coefficient of Restitution

Coefficient of restitution (C_r) is the change in kinetic energy of a particle when it collides with another object (static or kinetic). The importance of measuring coefficient of restitution is to accurately predict the deformation behavior and motion of the particles after collision with other grain particles or with rollers. In developing a DEM model to account for the stress and deformation produced in wheat kernels during milling, coefficient of restitution values help in determining the change in kinetic energy of the particles. A drop test as described by Bharadwaj and Smith (2010) was performed to measure the C_r of wheat mill stream particles. The 1st/2nd break stream and flour samples were compacted into tablets (diameter 9 ± 0.5 mm and thickness 3.5 ± 0.5 mm) using a custom made tablet press present at the Department of Grain Science and Industry. On about 250 mg of samples, compressional force of about 200-250 x 10^5 psi was applied through the press. To measure the coefficient of restitution, in a closed chamber, the samples (wheat kernels or tablets made from wheat mill streams and wheat flour; 25 replicates for each sample) were dropped from an initial height H_0, onto a steel platform. The tablets rebounded to a height H_1 after colliding with the surface. The complete motion of the sample was recorded by a camera (Exilim EX-F1, Casio Computer Co. Ltd., Tokyo, Japan) at 300 fps. Assuming a zero initial velocity of the sample, the coefficient of restitution was calculated as a function of the rebound height of the sample as given by Equation 3-4.

$$C_r = \sqrt{\frac{H_1}{H_0}} \qquad \textbf{3-4}$$

3.3.10 Statistical Analysis

Size, size distribution, density, and friction tests were performed in triplicate. The coefficient of restitution test was performed 25 times for samples from each mill stream without repeating the same sample. Wheat kernel hardness testing was carried out with a fixed weight of sample. Results were analyzed for statistical significance using SAS 9.3 (SAS Institute, Cary, NC, USA). The physical and mechanical properties were compared using the Tukey's Honestly Significant Difference Test using SAS.

3.4 Results and Discussions

Crude protein and fat content were lower for SRW samples compared to HRW and HRS samples, but the break stream crude fiber, ash content and starch content were higher (Table 3-1). There was no significant difference in the sample chemical composition except for the crude protein and break stream crude fiber content. The chemical composition of the break stream and flour depends on the mill operational parameters; hence, the composition of the wheat endosperm and bran also depends on the operational parameters. Furthermore, mill operators can vary the operational parameters to adjust the flour extraction rate, the load on the sifters, and the bran level in the flour, and that can also affect the chemical composition and quality of the break stream and flour.

Table 3-1: Proximate analysis of wheat mill break stream and flour[a]

	Crude Protein (w/w %)	Crude Fat (w/w %)	Crude Fiber (w/w %)	Ash (w/w %)	Starch (w/w %)
1st/2nd Break Stream					
HRW	11.46 (0.34) b	1.28 (0.21) a	2.22 (0.0) b	1.79 (0.05) a	58.10 (2.20) a
HRS	15.21 (0.13) a	1.35 (0.14) a	2.41 (0.23) ab	1.80 (0.12) a	60.17 (0.49) a
SRW	9.85 (0.11) c	1.24 (0.19) a	2.88 (0.02) a	1.89 (0.00) a	65.98 (3.08) a
Straight Grade Flour					
HRW	12.82 (0.01) b	0.39 (0.07) a	0.12 (0.09) a	0.65 (0.01) a	93.92 (3.18) a
HRS	16.58 (0.04) a	0.37 (0.04) a	0.27 (0.02) a	0.67 (0.04) a	89.27 (2.98) a
SRW	10.72 (0.06) c	0.33 (0.01) a	0.38 (0.06) a	0.57 (0.03) a	96.39 (2.82) a

[a] HRW = hard red winter; HRS = hard red spring, SRW = soft red winter. Values in parentheses are standard deviations. The same letter within the same column for a given sample indicates no significant difference ($p \geq 0.05$).

3.4.1 Single Kernel Characterization System

The hardness index is a parameter used to distinguish between hard and soft wheat classes. The hardness index of HRW and HRS wheat kernels was nearly three times that of SRW wheat kernels (**Error! Reference source not found.**). The difference in hardness index can be attributed to the difference in the starch-protein matrix in the kernel. However, there was no significant difference in the hardness index for all three wheat classes with moisture (**Error! Reference source not found.**). Similarly, the weight of individual kernels also varied slightly with moisture (**Error! Reference source not found.**), but this variation was significant for SRW wheat kernels, implying that water molecules could more easily migrate into the kernel due to the weak starch-protein matrix, resulting in an increase in weight. Hard wheat, having tightly integrated cell structures, results in higher hardness index values than soft wheat (Turnbull and Rahman, 2002).

Table 3-2: Wheat kernel characteristics

Moisture Content (% w.b.)	Hardness Index	Weight (mg)	Size (μm)
HRW			
12.10	62.14 (17.86) a	28.70 (9.80) a	2550 (400) a
14.35	64.39 (16.57) a	28.50 (9.10) a	2590 (400) a
15.93	62.97 (16.52) a	29.00 (8.50) a	2610 (410) a
HRS			
12.00	79.39 (17.63) a	27.60 (9.40) a	2620 (420) a
13.70	74.99 (18.51) b	27.90 (9.40) a	2620 (440) a
15.48	76.16 (17.40) ab	29.00 (10.60) a	2680 (430) a
SRW			
11.82	13.74 (22.97) b	32.80 (8.90) b	2640 (360) a
13.58	14.83 (21.71) b	34.90 (9.80) ab	2680 (340) a
15.70	18.45 (19.44) a	36.20 (10.00) a	2720 (360) a

[a]HRW = hard red winter; HRS = hard red spring, SRW = soft red winter. Values in parentheses are the average standard deviations of the replicates. The same letter in the same column for a given sample indicates no significant difference ($p \geq 0.05$).

3.4.2 Particle Size and Particle Size Distribution

The particle size of mill streams depends to a significant extent on the milling method and wheat type (Hareland, 1994). The primary purpose of first break milling is to break open the wheat kernel, yielding bran and endosperm particles with minimum bran breakage. This implies that 1st/2nd break would have a larger particle size and size distribution compared to the other mill stream products, since the primary composition is bran and flour. For the 1st/2nd break streams of the three different wheat classes, the SRW break stream had the smallest particle size, and the HRW break stream had the largest. This can be attributed to the difference in the hardness index of the different wheat classes and the difference in the breakage behavior of the two wheat classes. SRW wheat kernels, having the lowest hardness index, break into a greater proportion of smaller particles compared to hard wheat kernels (Fang and Campbell, 2002). Cohesion and agglomeration were not as evident in the HRW and HRS flours as they were in the SRW flour. The difference in mean particle size for each of the 1st/2nd break streams can be attributed to the difference in kernel hardness (Dziki, 2008).

From the particle size of the flour, obtained using the laser diffraction technique, we observed that there was no significant difference in the mean particle size of flour with moisture content within the same wheat class, even though the particle size increased (Table 3-3). The average particle size ranged from 37 to 52 μm for the flours from the evaluated wheat classes. From the cumulative distribution of the laser diffraction analysis, it was observed that at least 90% of the flour particles were in the range of 2 to 50 μm (Figure 3-1). Glenn and Saunders (1990) reported that starch-protein adhesion and intracellular spaces varied within each wheat class due to the starch-protein matrix continuity in the endosperm, resulting in a variation in the particle size distributions of different wheat classes. As a result, a wide distribution of particle sizes was noticed, ranging from 2 to 400 μm. The mean particle size of the SRW flour was higher or comparable with the HRW and HRS flour particles due to higher cohesion between the SRW flour particles (Neel and Hoseney, 1984; Patwa et al., 2014). Similar results were observed by Hareland (1994) in a study on the evaluation of particle size of flour from different wheat classes.

Table 3-3: Particle size and size distribution of wheat mill break stream and straight grade flour at different moisture content[a]

Target Moisture content (%w.b.)	Actual Moisture Content (%w.b.)	Average Particle Size (μm)	Target Moisture content (%w.b.)	Actual Moisture Content (%w.b.)	Average Particle Size (μm)
HRW Break Stream			HRW Flour		
12.00	11.36	565.58 (7.14) cA	12.00	12.48	37.9 (2.6) aB
14.00	13.87	590.11 (3.53) bA	14.00	13.55	39.8 (2.1) aB
16.00	15.17	800.42 (12.38) aA	16.00	15.80	41.2 (0.3) aC
HRS Break Stream			HRS Flour		
12.00	12.83	638.82 (50.49) bA	12.00	11.94	50.3 (2.8) aA
14.00	14.64	495.59 (4.22) bB	14.00	14.23	52.6 (5.9) aA
16.00	16.72	531.77 (28.66) aB	16.00	15.55	57.2 (1.0) aA
SRW Break Stream			SRW Flour		
12.00	12.06	464.98 (21.19) cB	12.00	11.46	47.1 (4.8) aAB
14.00	14.06	424.92 (37.23) bC	14.00	13.61	51.5 (3.7) aA
16.00	15.44	355.72 (30.16) aC	16.00	15.67	52.1 (0.8) aB

[a] HRW = hard red winter; HRS = hard red spring, SRW = soft red winter. Values in parentheses are standard deviations. The same lowercase letter in the same column for a given sample indicates no significant difference ($p \geq 0.05$); the same uppercase letter in the same column indicates no significant difference ($p \geq 0.05$) at given moisture content across wheat classes.

[b] Particle size measured using laser diffraction particle size analyzer.

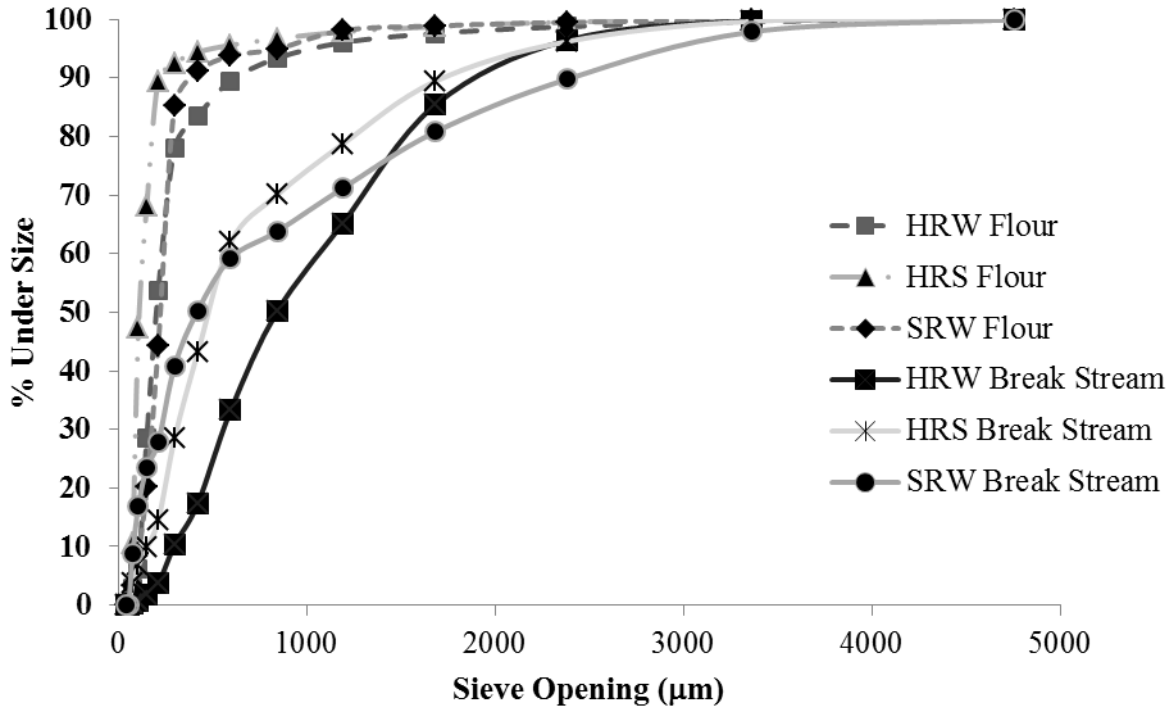

Figure 3-1: Cumulative particle size distribution of wheat mill break streams and flour at 16% moisture content

3.4.3 Bulk Density

There was a decrease in bulk density of wheat kernels by approximately 20 kg/m3 with increasing moisture from 12% to 16% for all three wheat classes (Table 3-4). The decrease in density corresponded to the increase in mass due to water addition. This increase being lower than the corresponding increase in volume occupied by the grains resulted in decrease in the overall bulk density since the density is inversely proportional to volume. Similar linear negative relationships of bulk density to moisture content have been found for different seeds and grains, such as barley and jatropha seed (Garnayak et al., 2008; Ozturk and Esen, 2008). The bulk densities of the 1st/2nd break stream and flour did not display a similar trend (Table 3-5 and Table 3-6). Instead, the bulk density of the break stream increased with increasing moisture content, but the increase was not statistically significant ($p \geq 0.05$; Table 3-5). This observed trend was due to the composition of the 1st/2nd break stream, which comprised of a mix of bran

and flour particles. As a result, addition of water led to swelling of the endosperm particles, resulting in a lower increase in volume compared to the mass of the break stream.

However flour from all three wheat classes did not display a definite trend. In case of HRW and SRW wheat flour, the density increased from 12% to 16% but in case of HRS wheat flour, decreasing values of bulk density were observed. No definite reasoning could be found the decreasing trend displayed by HRS flour, but Subramanian and Viswanathan (2007) also reported increase in the bulk density of different millet flours with moisture content.

3.4.4 Tapped Density

The tapped or compressed bulk density of wheat kernels decreased with an increase in moisture (Table 3-4). This was possibly due to the increase in mass of the material with moisture addition. The tapping motion resulted in a reduction of the volume occupied by the samples because the grains repack themselves into void spaces. Apparently, this decrease in volume due to tapping was less than the increase in grain mass due to moisture addition, resulting in the decreased tapped density.

While the wheat kernels displayed a negative relationship between tapped density and moisture content, this was not the case for the 1st/2nd break stream and flour samples. Comparing the tapped density values for the different break streams at each moisture level, we observed the values did not show any specific trend across wheat classes (Table 3-5). This behavior can be attributed to the mixed composition of the break stream, which contained partially milled bran particles that had been separated from the endosperm as well as endosperm fragments. Thus, the break stream was comprised of both large-size bran particles as well as smaller endosperm particles. As a result, during tapping of the samples, the smaller flour particles settle into the void spaces, resulting in a volume decrease. However, due to the presence of larger bran particles, the decrease in volume of the bulk sample was not significant. Because the quantity and percentage of bran and endosperm in a given replicate is highly variable, the trend was not definite, and the standard deviation was large. For the HRS and SRW flours, the tapped density decreased with increasing moisture (Table 3-5). The wider particle size distribution of the flour samples could have led to the large standard deviations observed for the tapped density values.

Table 3-4: Property values of HRW, HRS and SRW wheat kernels at different moisture contents[a]

Target Moisture content (% w.b.)	Actual Moisture Content (% w.b.)	Bulk Density (kg m^{-3})	Tapped Density (kg m^{-3})	True Density (kg m^{-3})	Young's Modulus (MPa)	Coefficient of Static Friction	Coefficient of Rolling Friction	Coefficient of Restitution
HRW								
12.00	12.10	779.07 (0.10) aA	820.94 (4.14) aA	1422.71 (1.66) aB	15.88 (2.53) aA	0.38 (0.03) aA	0.19 (0.01) aA	0.33 (0.03) aB
14.00	14.35	767.74 (0.47) bB	814.21 (1.94) aA	1419.86 (0.77) bB	14.87 (1.38) aA	0.39 (0.03) aA	0.19 (0.04) aA	0.32 (0.04) aA
16.00	15.93	760.26 (1.60) cA	803.10 (4.51) bA	1416.40 (2.29) cB	12.75 (0.50) aA	0.40 (0.03) aA	0.20 (0.01) aA	0.32 (0.03) aA
HRS								
12.00	12.00	783.85 (1.97) aA	823.38 (5.67) aA	1426.05 (0.76) aA	16.52 (1.05) aA	0.38 (0.03) aA	0.17 (0.02) bA	0.34 (0.03) aB
14.00	13.70	778.70 (0.41) bA	816.00 (3.32) aA	1422.12 (1.34) bA	15.35 (0.64) abA	0.39 (0.02) aA	0.19 (0.003) abA	0.33 (0.02) aA
16.00	15.48	762.73 (2.56) cA	806.49 (9.79) aA	1421.08 (0.98) bA	13.83 (0.21) bA	0.41 (0.04) aA	0.24 (0.02) aA	0.33 (0.03) aA
SRW								
12.00	11.82	760.53 (3.07) aB	797.20 (3.81) aB	1383.43 (1.67) aC	14.75 (0.93) aA	0.39 (0.03) bA	0.18 (0.01) bA	0.38 (0.05) aA
14.00	13.58	756.28 (0.89) aC	787.51 (2.93) abB	1378.33 (1.01) bC	13.68 (0.21) aA	0.43 (0.02) abA	0.18 (0.02) bA	0.35 (0.03) abA
16.00	15.70	743.08 (1.39) bB	780.39 (6.39) bB	1371.4 (1.8) cC	12.47 (1.70) aA	0.47 (0.03) aA	0.24 (0.01) aA	0.33 (0.02) bA

[a]HRW = hard red winter; HRS = hard red spring, SRW = soft red winter. Values in parentheses are standard deviations. The same lowercase letter in the same column for a given sample indicates no significant difference ($p \geq 0.05$); the same uppercase letter in a column indicates no significant difference ($p \geq 0.05$) between wheat class sample comparisons at given moisture content.

Table 3-5: Property values of HRW, HRS and SRW 1st break stream samples at different moisture contents[a]

Target Moisture content (% w.b.)	Actual Moisture Content (% w.b.)	Bulk Density (kg m^{-3})	Tapped Density (kg m^{-3})	True Density (kg m^{-3})	Young's Modulus (MPa)	Coefficient of Static Friction	Coefficient of Rolling Friction	Coefficient of Restitution
HRW								
12.00	11.36	457.80 (3.19) bA	495.46 (17.84) bB	1453.26 (0.44) aB	0.39 (0.06) aA	0.33 (0.01) bA	0.17 (0.01) bC	0.27 (0.03) bA
14.00	13.87	487.33 (5.10) abA	591.08 (49.86) aA	1449.86 (1.23) bB	0.43 (0.16) aA	0.36 (0.01) abA	0.18 (0.00) bB	0.30 (0.02) abA
16.00	15.17	511.44 (28.18) aA	562.70 (6.76) abB	1430.89 (1.77) cB	0.52 (0.14) aA	0.37 (0.02) aA	0.23 (0.02) aB	0.31 (0.02) aA
HRS								
12.00	12.83	459.98 (8.38) aA	590.65 (57.65) aA	1442.43 (1.47) aC	0.17 (0.09) aB	0.33 (0.03) aA	0.21 (0.01) bB	0.27 (0.03) bA
14.00	14.64	458.35 (4.28) aB	535.14 (38.40) aA	1437.39 (2.51) aC	0.25 (0.06) aAB	0.36 (0.01) aA	0.26 (0.03) bA	0.30 (0.03) abA
16.00	16.72	472.53 (26.50) aA	551.28 (11.09) aB	1430.89 (1.77) bB	0.41 (0.26) aA	0.37 (0.04) aA	0.31 (0.03) aA	0.32 (0.04) aA
SRW								
12.00	12.06	463.40 (10.26) aA	574.79(10.89)bAB	1464.15 (1.59) aA	0.06 (0.01) bB	0.34 (0.03) aA	0.26 (0.02) bA	0.25 (0.02) bA
14.00	14.06	447.97 (5.22) aB	555.82 (24.97) bA	1457.36 (0.60) bA	0.08 (0.005) bB	0.37 (0.01) aA	0.26 (0.01) abA	0.29 (0.04) aA
16.00	15.44	476.72 (16.75) aA	621.70 (7.65) aA	1450.51 (1.28) cA	0.12 (0.01) aA	0.37 (0.04) aA	0.31 (0.03) aA	0.30 (0.03) aA

[a]HRW = hard red winter; HRS = hard red spring, SRW = soft red winter. Values in parentheses are standard deviations. The same lowercase letter in the same column for a given sample indicates no significant difference ($p \geq 0.05$); the same uppercase letter in a column indicates no significant difference ($p \geq 0.05$) between wheat class sample comparisons at given moisture content.

Table 3-6: Property values of HRW, HRS and SRW straight grade wheat flour at different moisture contents[a]

Target Moisture content (% w.b.)	Actual Moisture Content (% w.b.)	Bulk Density (kg m^{-3})	Tapped Density (kg m^{-3})	True Density (kg m^{-3})	Young's Modulus (MPa)	Coefficient of Static Friction	Coefficient of Rolling Friction	Coefficient of Restitution
HRW								
12.00	12.48	519.75 (10.70) bA	693.29 (37.86)aAB	1475.51 (0.27) aB	0.12 (0.03) bB	0.45 (0.03) aA	0.50 (0.02) aA	0.26 (0.02) bB
14.00	13.55	533.86 (8.20) bB	691.29 (4.87) aB	1470.33 (0.70) bB	0.21 (0.01) bA	0.43 (0.04) aA	0.55 (0.03) aA	0.27 (0.02) abB
16.00	15.80	570.50 (1.94) aA	725.58 (2.13) aA	1467.64 (1.28) cB	1.55 (0.63) aA	0.45 (0.03) aA	0.51 (0.02) aA	0.30 (0.04) aB
HRS								
12.00	11.94	572.18 (5.55) aA	730.42 (3.02) aA	1465.34 (0.27) aC	0.87 (0.41) bAB	0.34 (0.02) bB	0.32 (0.02) aC	0.30 (0.01) bA
14.00	14.23	566.93 (2.48) aA	701.50 (3.41) bA	1460.16 (0.45) bC	1.87 (0.47) abA	0.36 (0.01) aB	0.50 (0.02) aA	0.31 (0.03) bA
16.00	15.55	565.63 (2.54) aA	698.97 (3.24) bB	1449.58 (1.12) cC	3.31 (0.84) aA	0.41 (0.02) aA	0.52 (0.01) bA	0.38 (0.04) aA
SRW								
12.00	11.46	440.07 (3.11) bC	653.41 (7.33) aB	1488.27 (0.96) aA	0.06 (0.03) aA	0.44 (0.02) aA	0.39 (0.01) bB	0.28 (0.02)aAB
14.00	13.61	440.27 (5.98) bC	630.46 (2.21) bC	1476.73 (1.35)bA	0.05 (0.02) aA	0.45 (0.01) aA	0.40 (0.05) abB	0.30 (0.02) aA
16.00	15.67	460.51 (1.25) aB	621.68 (8.03) bC	1470.10 (0.95) cA	0.08 (0.02) aA	0.47 (0.02) aA	0.48 (0.03) aA	0.31 (0.07) aB

[a] HRW = hard red winter; HRS = hard red spring, SRW = soft red winter. Values in parentheses are standard deviations. The same lowercase letter in the same column for a given sample indicates no significant difference ($p \geq 0.05$); the same uppercase letter in a column indicates no significant difference ($p \geq 0.05$) between wheat class sample comparisons at given moisture content.

3.4.5 True Density

The true density of all samples, (wheat kernels, break streams, and flour) decreased with increasing moisture content (Table 3-4 through Table 3-6). The addition of moisture to the kernels increased the mass as well as the volume. The increase in volume influenced the true density of the kernels more than the increasing mass did and resulted in a significant decrease in true density in the range of 10 to 20 kgm^{-3}. We observed a lower true density value for SRW wheat kernels compared to the hard wheat kernels. Urena et al. (2002) reported that the average true density of hard wheat at 9.09% moisture was 1420 kgm^{-3}. Although the density values of soft wheat reported by Chang (1988) were higher than the values obtained in this study, those for hard wheat were in a similar range.

For the break stream and flour samples, there was a significant decrease ($p < 0.05$) in the true density with the change in moisture content (Table 3-5). Addition of water causes starch granules to swell, increasing their volume and decreasing their density. Because flour particles are made up of starch and protein, the decrease in density could be due to swelling of the starch-protein matrix with addition of water.

3.4.6 Young's Modulus

Young's modulus measures the stress-strain characteristics of a material. These characteristics, along with other mechanical properties, can be used to predict the breakage behavior and describe the grinding process for the material. The Young's modulus value for wheat kernel samples decreased with increasing moisture for HRS wheat kernels but did not show a significant trend for HRW and SRW wheat kernels (Table 3-4). The Young's modulus value decreased because addition of moisture made the endosperm softer while toughening the pericarp to enhance separation of the endosperm and bran (Pomeranz and Williams, 1990). Kernel elasticity decreased and resulted in a decrease of Young's modulus (Dziki et al., 2010; Glenn et al., 1991). This implies that increasing the moisture enables the separation of bran from the endosperm, and this is the reason for tempering wheat grains prior to milling. Similar observations were reported by Dziki et al. (2010) for individual wheat kernels and by Wozniac and Styk (1996) for barley grains.

The 1st/2nd break streams conversely showed an increase in Young's modulus with moisture (Table 3-5). Other than softening the endosperm, the other objective of tempering

wheat prior to milling is to keep the bran intact to enable easy separation during the sifting process. We observed an increase in the Young's modulus values for the break stream ($p < 0.05$). Since the break stream is made up of bran and flour, the adhesion and cohesion forces are not strong due to the differences in particle sizes. Therefore, with the addition of moisture to the sample, the volume of the break stream particles increased, resulting in a smaller strain produced for the same applied stress. Hence, the Young's modulus increased with an increase in the moisture content.

Increasing moisture did not have a significant effect ($p \geq 0.05$) on the Young's modulus of soft wheat flour (Table 3-6). Increase in the moisture content of flour increased the interaction strength between particles. As a result, when stress was applied, the strain produced in flour decreased by a smaller margin due to the compact and cohesive nature of the flour particles, resulting in a small increase in Young's modulus. Hence, moisture did not have a significant effect on the Young's modulus of SRW flour ($p \geq 0.05$).

3.4.7 Coefficients of Static and Rolling Friction

When a wheat kernel comes into contact with the break rolls during milling, it offers some resistance to the shear and compressional forces of the rolls. In DEM model development, the resistance force offered by the wheat kernel will be determined using the data from the friction coefficient values between the grain and the roll surface.

The coefficient of friction values for wheat kernels from the three classes ranged from 0.38 to 0.47 for static friction and from 0.17 to 0.24 for rolling friction (Table 3-4). Although the friction coefficients appeared to increase with moisture addition, the effect of moisture was not significant ($p \geq 0.05$) although Brubaker and Pos (1965) reported that the coefficient of friction was significantly influenced by kernel moisture content. Babić et al. (2011) reported that wheat coefficient of friction values ranged from 0.32 to 0.36 depending on the wheat class. Similar results of a linear increase in friction coefficient with moisture were reported by other researchers for grains such as pulses (Amin et al., 2005).

Moisture content did not significantly affect ($p \geq 0.05$) the coefficients of static friction of the break stream samples (Table 3-5). However, there was a significant effect ($p < 0.05$) of moisture on the rolling friction coefficient of the break stream samples. This can be attributed to the compositional variability and the wide particle size distribution of the break stream samples.

Consequently, the coefficients of static and rolling friction of wheat flour were in the same range (Table 3-6), unlike wheat kernels and break streams, for which the rolling friction coefficients were lower than the static friction coefficients. This is due to the fact that flour particles are smaller than wheat kernels and break stream particles. Therefore, more compaction takes place in flour on application of force, resulting in a higher rolling friction coefficient. For wheat flour, both friction coefficients increased with moisture content. Subramanian and Viswanathan (2007) also reported an increase in friction coefficient with moisture content for millet flours.

3.4.8 Coefficient of Restitution

In case of break streams and flour, only the compact tablets that rebounded back without any angular movement and had a direct impact on the metal surface were selected for calculation purposes. While in case of wheat kernels, care was taken to drop each grain in the same orientation.

The coefficient of restitution of wheat kernels from the three classes ranged from 0.3 to 0.4 (Table 3-4). There was no significant effect of moisture on the coefficient of restitution for HRW and HRS wheat kernels. However, for SRW wheat kernels, there was a significant decrease in the coefficient of restitution with increasing moisture, which could be attributed to the lower kernel hardness of soft wheat kernels. Similar observations were made by Ozturk et al. (2010) for chick pea and lentil seeds; they reported that the coefficient of restitution depended on the moisture content and drop height. However, in our experiments, the drop height was kept constant in order to simulate the fall of wheat kernels from the feed hopper onto the break roll during the milling process.

Unlike wheat kernels, the restitution value for the break streams and flour generally increased with increasing moisture (Table 3-5 and Table 3-6). While the coefficient of restitution increased, the variation with moisture content within a wheat class was low. The values ranged from 0.25 to 0.30 for the break stream and from 0.24 to 0.40 for flour. The values for the break stream tablets were lower than for the flour tablets due to the differences in composition and particle size distribution of the materials from which the tablets were prepared. In the case of the SRW break stream and flour tablets, there was no variation in the coefficient of restitution values with moisture content, possibly because of the compact and cohesive nature of the SRW

endosperm particles. However, in the case of the HRW and HRS break stream and flour tablets, there was significant ($p < 0.05$) variation with moisture content.

3.5 Conclusion

In determining the different physical and material properties of wheat mill streams, it was observed that moisture content had a significant effect on some physical properties of the mill streams and flour (i.e., particle size and size distribution, bulk density, and tapped density) that was greater than the effect on material properties (i.e., Young's modulus, coefficients of friction, and coefficient of restitution). The variation in properties of the mill streams from different wheat classes can be attributed to differences in hardness, milling method, and growing conditions. These physical and material property values, namely, particle size and size distribution, bulk density, coefficients of rolling and static friction, Young's modulus, and coefficient of restitution, will be used as input parameters in developing a DEM model of the break roll milling process of wheat. Using these properties, spherical particles that simulate wheat kernels and wheat mill stream particles in their behavior and properties will be created and used in the model. By taking into account the variability of these properties for different wheat classes, we can accurately predict the milling of wheat during first break milling.

3.6 References

AACC. (1999). 76-13.01: Total starch assay procedure (megazyme amyloglucosidase/α-amylase method). St. Paul, Minn.: AACC International.

Amin, M. N., Ahammed, S., Roy, K. C., & Hossain, M. A. (2005). Coefficient of friction of pulse grains on various surfaces at different moisture content. *International Journal of Food Properties, 8*(1), 61-67.

AOAC. (2000). 925.10: Solids (total) and moisture in flour. In *Official Methods of Analysis* (17 ed.). Gaithersburg, Md.: AOAC International

AOAC. (2006a). 920.39: Fat (crude) or ether extract in animal feed. In *Official Methods of Analysis* (17 ed.). Gaithersburg, Md.: AOAC International.

AOAC. (2006b). 934.01: Moisture in animal feed: Loss on drying at 95°C to 100°C. In *Official Methods of Analysis* (17 ed.). Gaithersburg, Md.: AOAC International.

AOAC. (2006c). 942.05: Ash in animal feed. In *Official Methods of Analysis* (17 ed.). Gaithersburg, Md.: AOAC International.

AOAC. (2006d). 978.10: Fiber (crude) in animal feed and pet food. In *Official Methods of Analysis* (17 ed.). Gaithersburg, Md.: AOAC International.

AOAC. (2006e). 984.13: Protein (crude) in animal feed, forage (plant tissue), grain, and oil seeds. In *Official Methods of Analysis* (17 ed.). Gaithersburg, Md.: AOAC International.

ASABE. (2008). S 319.4: Method of determining and expressing fineness of feed materials by sieving. St. Joseph, Mich.: ASABE.

Babić, L., Babić, M., Turan, J., Matic-Kekic, S., Radojcin, M., Mehandzic-Stanisic, S., Pavkov, I., & Zoranovic, M. (2011). Physical and stress-strain properties of wheat (*Triticum aestivum*) kernel. *Journal of the Science of Food and Agriculture, 91*(7), 1236-1243.

Bharadwaj, R., Smith, C., & Hancock, B. C. (2010). The coefficient of restitution of some pharmaceutical tablets/compacts. *International Journal of Pharmaceutics, 402*(1-2), 50-56.

Boac, J. M., Casada, M. E., Maghirang, R. G., & Harner III, J. P. (2010). Material and interaction properties of selected grains and oilseeds for modeling discrete particles. *Transactions of the ASABE, 53*(4), 1201-1216.

Brubaker, J. E., & Pos, J. (1965). Determining static coefficients of friction of grains on structural surfaces. *Transactions of the ASAE, 8*(1), 53-55.

Campbell, G. M., Fang, C., & Muhamad, I. I. (2007). On predicting roller milling performance: VI. Effect of kernel hardness and shape on the particle size distribution from first break milling of wheat. *Food and Bioproducts Processing, 85*(C1), 7-23.

CFR (2013). 21 CFR 137.105: Requirements for specific standardized cereal flours and related products. Washington, D. C.: Code of Federal Regulations.

Chang, C. S. (1988). Measuring density and porosity of grain kernels using a gas pycnometer. *Cereal Chemistry, 65*(1), 13-15.

Cleary, P. W. (2001). Recent advances in DEM modelling of tumbling mills. *Minerals Engineering, 14*(10), 1295-1319.

Delwiche, S. R. (2000). Wheat endosperm compressive strength properties as affected by moisture. *Transactions of the ASAE, 43*(2), 365-373.

Dziki, D. (2008). The crushing of wheat kernels and its consequence on the grinding process. *Powder Technology, 185*(2), 181-186.

Dziki, D., & Laskowski, J. (2004). Influence of kernel size on grinding process of wheat at respective grinding stages. *Polish Journal of Food and Nutrition Sciences, 13*(1), 29-33.

Dziki, D., Laskowski, J., Siastala, M., & Biernacka., B. (2010). Influence of moisture content on the wheat kernel mechanical properties determined on the basis of shear test. *International Agrophysics, 24*(3), 237-242.

Fang, C. Y., & Campbell, G. M. (2002). Effect of roll fluting disposition and roll gap on breakage of wheat kernels during first-break roller milling. *Cereal Chemistry, 79*(4), 518-522.

Fang, Q. (1995). Effects of physical properties of wheat and operational parameters of roller mills on size reduction. Manhattan, Kans.: Kansas State University, Department of Grain Science and Industry.

Fang, Q., Biby, G., Haque, E., Hanna, M. A., & Spillman, C. K. (1998). Neural network modeling of physical properties of ground wheat. *Cereal Chemistry, 75*(2), 251-253.

Garnayak, D. K., Pradhan, R. C., Naik, S. N., & Bhatnagar, N. (2008). Moisture-dependent physical properties of Jatropha seed (Jatropha curcas L.). *Industrial Crops and Products, 27*(1), 123-129.

Glenn, G. M., & Saunders, R. M. (1990). Physical structural properties of wheat endosperm associated with grain texture. *Cereal Chemistry, 67*(2), 176-182.

Glenn, G. M., Younce, F. L., & Pitts, M. J. (1991). Fundamental physical-properties characterizing the hardness of wheat endosperm. *Journal of Cereal Science, 13*(2), 179-194.

Hareland, G. A. (1994). Evaluation of flour particle-size distribution by laser diffraction, sieve analysis, and near-infrared reflectance spectroscopy. *Journal of Cereal Science, 20*(2), 183-190.

Horiba. (2008). User manual: LA-910 laser scattering particle size distribution analyzer. Kyoto, Japan: Horiba.

Jayas, D. S., & Cenkowski, S. (2007). Grain property values and their measurement. In A. S. Majumdar (Ed.), *Handbook of Industrial Drying* (pp. 575-600). Boca Raton, Fla.: CRC Press.

Jirsa, O., Hruskova, M., & Svec, I. (2008). Near-infrared prediction of milling and baking parameters of wheat varieties. *Journal of Food Engineering, 87*(1), 21-25.

Kingsly, A. R. P., & Ileleji, K. E. (2009). Sorption isotherm of corn distillers dried grains with solubles and its prediction using chemical composition. *Food Chemistry, 116*(4), 939-946.

Mateos-Salvador, F., Sadhukhan, J., & Campbell, G. M. (2011). The normalised Kumaraswamy breakage function: A simple model for wheat roller milling. *Powder Technology, 208*(1), 144-157.

Neel, D. V., & Hoseney, R. C. (1984). Sieving characteristics of soft and hard wheat flours. *Cereal Chemistry, 61*(4), 259-261.

Niernberger, F. F. (1966). Roll diameter and speed: Their effects on first break grinding of wheat. Manhattan, Kans.: Kansas State University, Department of Grain Science and Industry.

Oleson, B. T. (1994). World wheat production, utilization, and trade. In W. Bushuk, & V. F. Rasper (Eds.), *Wheat: Production, Properties and Quality* (pp. 1-11). London, U.K.: Blackie Academic and Professional.

Ozturk, T., & Esen, B. (2008). Physical and mechanical properties of barley. *Agricultura Tropica et Subtropica, 41*(3), 117-121.

Ozturk, I., Kara, M., Uygan, F., & Kalkan, F. (2010). Restitution coefficient of chick pea and lentil seeds. *International Agrophysics, 24*(2), 209-211.

Pasikatan, M. C., Milliken, G. A., Steele, J. L., Haque, E., & Spillman, C. K. (2001). Modeling the energy requirements of first-break grinding. *Transactions of the ASAE, 44*(6), 1737-1744.

Patwa, A., Malcolm, B., Wilson, J., & Ambrose, R. P. (2014). Particle size analysis of two distinct classes of wheat flour by sieving. *Transactions of the ASABE, 57*(1), 151-159.

Pomeranz, Y., & Williams, P. C. (1990). Wheat hardness: Its generic, structural, biochemical background, measurement, and significance. In Y. Pomeranz (Ed.), *Advances in Cereal Science and Technology*, Vol. 10 (pp. 471-557). St. Paul, Minn.: AACC International.

Posner, E. S., & Hibbs, A. N. (2005). *Wheat flour milling*, second edition. St. Paul, Minn.: AACC International.

Subramanian, S., & Viswanathan, R. (2007). Bulk density and friction coefficients of selected minor millet grains and flours. *Journal of Food Engineering, 81*(1), 118-126.

Turnbull, K. M., & Rahman, S. (2002). Endosperm texture in wheat. *Journal of Cereal Science, 36*(3), 327-337.

Urena, M. O., Galvan, M. G., & Teixeira, A. A. (2002). Measurement of aggregate true particle density to estimate grain mixture composition. *Transactions of the ASAE, 45*(6), 1925-1928.

Wozniak, W., & Styk, W. (1996). Internal damage to wheat grain as a result of wetting and drying. *Drying Technology, 14*(2), 349-365.

Wrigley, C. W. (2009). Wheat: A unique grain for the world. In K. A. Khan, & P. R. Shewry (Eds.), *Wheat Chemistry and Technology* (pp. 1-17). St. Paul, Minn.: AACC International.

Yap, S. F., Adams, M. J., Seville, J. P., & Zhang, Z. (2008). Single and bulk compression of pharmaceutical excipients: Evaluation of mechanical properties. *Powder Technology, 185*(1), 1-10.

Zoerb, G. C., & Hall, C. W. (1960). Some mechanical and rheological properties of grains. *Journal of Agricultural Engineering Research, 5*(1), 83-93.

Chapter 4 - DEM Model of 1st Break Wheat Milling using a Single Sphere Approach

The preliminary results were presented at a conference, with the citation below.

Conference presentation:

Patwa, A., Ambrose, K . 2014. Discrete Element Method Modeling of 1st Break Wheat Milling Process using a Single-Sphere Approach. World Congress of Particle Technology, May, 2014. Beijing, China. (Oral)

4.1 Introduction

The DEM is an extensively used modeling technique developed by Cundall and Strack primarily to model rock fracture mechanics (Cundall & Strack, 1979). Developed as an aid to model granular assemblies, DEM has wide applicability ranging from chemical and pharmaceutical industries to geomechnical industries. Over the past two decades, this method has been used quite extensively in modeling granular assemblies of food materials (Coetzee et al., 2010). Common application of DEM in the grain industry has involved modeling excavator bucket filling (Coetzee et al., 2007), commingling of grains in bucket elevators (Boac et al., 2010), and in the bulk handling and storage of cereal grains (Gonzalez-Montellano et al., 2012). But, the studies have been limited to mostly handling of grains. Another common application of DEM is to study the size reduction and breakage of granular material and agglomerates especially in a ball mill (Metzger & Glasser., 2013) and SAG mills (Cleary, 2001).

Roller milling of wheat is a multi-operation and multi-step process involving several break roll, reduction roll, sifting and purifying systems. Various studies have modeled the effect of different physical and mechanical parameters on the milling process (Fang et al., 1998; Pasikatan et al., 2001; Dziki, 2008; Campbell et al., 2001). Modeling techniques that have been tested include neural network models (Fang et al., 1998), population based models (Pasikatan et al., 2001), regression models (Dziki, 2008), breakage function models (Campbell et al., 2001), and breakage matrix approach (Fistes & Tanovic, 2006) for predicting the first break milling. The first break, which opens the wheat kernel, enables the separation of bran and endosperm portions of the wheat kernel, is the most important operation during wheat milling. In addition, the objective during first break also includes that the bran is not crushed or shattered, to

minimize bran contamination in flour. Majority of the reported studies are statistical models and they do not take into consideration the mechanical properties and non-uniformity in wheat kernels. But, DEM technique takes into consideration the physical and mechanical properties variability in the material.

The objective of this research is to develop a DEM model of the 1st break wheat milling process using a single sphere approach with the sphere representing wheat kernel.

4.2 Materials and Methods

4.2.1 Samples

Samples of hard red winter (HRW) wheat conditioned to 12%, 14% and 16% moisture content (wet basis) and the 1st break of the milled wheat at the above moisture levels were used for the model development. The physical and mechanical properties needed as input parameters in the model were previously measured (Patwa et al., 2014) and are given in Table 4-1.

4.2.2 Creating Geometry for the Simulation

The 1st break roll stand geometry was created in computer aided design software, AutoCAD 2013 (Autodesk Inc. CA, USA). The specifications of roll stand present at the Hall Ross Flour Mill (Department of Grain Science and Industry, Kansas State University) were used to create the model roll geometry (Table 4-1). The geometry, drawn using AutoCad, was imported into EDEM (DEM Solutions, Edinburgh, UK) as an *.iges* extension file (Figure 4-1 and Figure 4-2).

Figure 4-1: 1st break roll stand geometry

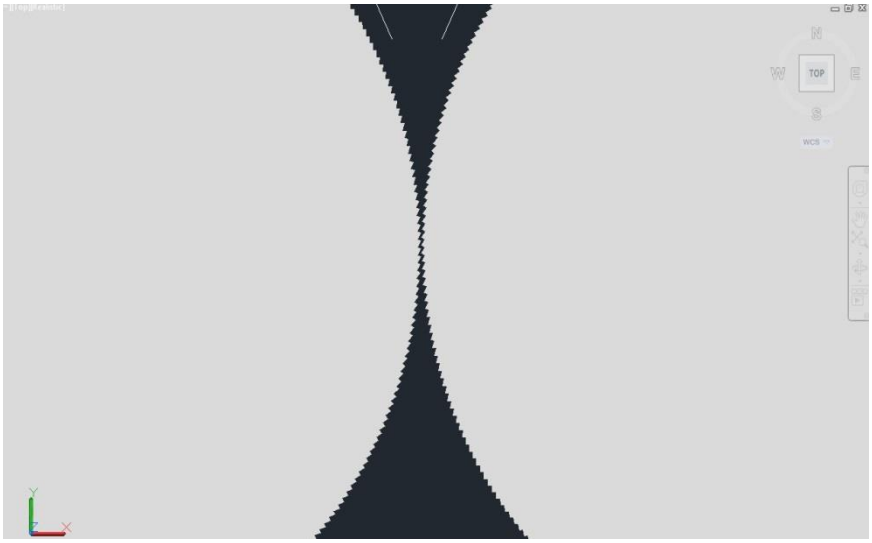

Figure 4-2: Dull-to-Dull roll disposition of 1st break roll stand geometry

The rolls were given rotation parameters to rotate at the specified speed maintaining the speed differential of 2.5:1 with a dull-to-dull grinding action. This creation of geometry with actual mill parameters enabled simulating an industrial milling process.

Table 4-1: 1st break roll stand dimensions used for simulation

Roll diameter, mm	250
Roll length, mm	800
Roll gap, mm	0.05
Roll speed, fast/slow, rpm	350/140
Speed differential, fast:slow roll	2.5:1
Grinding action	Dull-to-Dull
Flutes on circumference	350
Flutes per centimeter	4.5

4.2.3 Discrete Element Method (DEM)

The DEM simulations and model development were carried out using EDEM 2.6 software (DEM Solutions Ltd., Edinburgh, UK) installed in an Intel Core 2 Duo processor with a 4 GB RAM and 64-bit Windows 7 professional operating system. The DEM working principle is discussed in detail in Chapter 2. The discussion here is restricted to the operation of the model and the steps taken to simulate the process.

4.2.3.1 Creating Particles

The first step in developing a DEM model, of any process, is to create particles and assign these particles with physical and mechanical properties of the material being modeled. For the first approximation of this study, the wheat kernels and break stream particles were assumed to be spherical in shape. Here onwards, the wheat kernel and 1st break particles created in the model will be referred to as whole and fraction respectively. The whole and fraction particles created were given a definite radius and size distribution based on the measured values. The mean values for the particle density, shear modulus, Poissons ratio, coefficient of static and rolling friction, and coefficient of restitution were also given as inputs to the model for creation of these particles. The use of this set of selected properties enabled characterizing the whole and fraction particles as HRW wheat kernels and break stream particles respectively. The values used for all the property inputs were measured (Patwa et al., 2014b), except for the Poissons ratio and shear modulus, for which values available in published literature were used (Markauskas et al., 2010; Sarnavi et al., 2013; Weigler et al., 2012) as listed in Table 4-2.

4.2.3.2 Creating Custom Factory for Particle Cluster Formation

It is known that the wheat kernel is comprised of endosperm, bran and germ layers. For the purpose of this model, a spherical shaped cluster was created, comprised of individual 1st break fraction particles glued together as shown in Figure 4-3, representing the different layers of the wheat kernel. This cluster of fraction particles bonded together is equivalent to a wheat kernel represented by the whole particle.

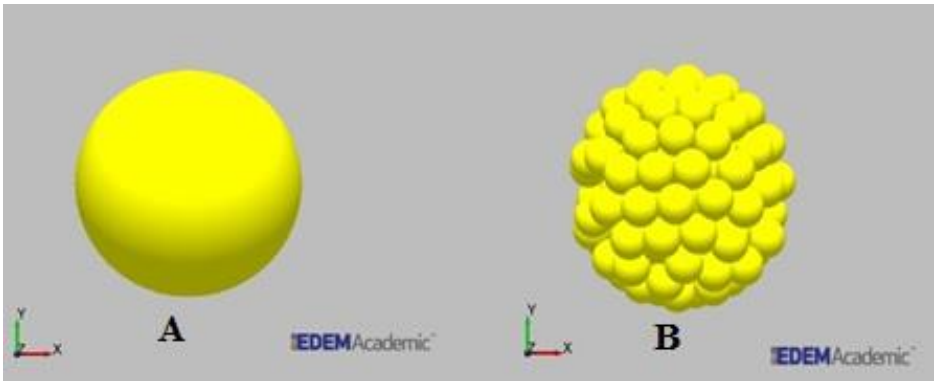

Figure 4-3: A) Single wheat kernel; B) Cluster made up of 1st break fraction particles;

To create this cluster of fraction particles, a custom factory was defined in EDEM. The purpose of creating the custom factory was to achieve the desired spherical shape of the cluster. The following steps were followed in EDEM to create a custom factory.

i) Create two cylinders around the origin one inside the other, large enough to fit 'whole' particles. The outside cylinder is the container and the inside cylinder is the particle factory to create the fraction particles.

ii) Define the fraction particle with the given properties and radius and a contact radius slightly larger than the physical radius.

iii) Define the particle factory for the fraction particles with no size distribution but instead a fixed size since the cluster is made up of uniformly sized fraction particles.

iv) Begin the simulation and fill up the outer cylinder with the fraction particles.

v) Upon completion of the simulation, import a spherical geometry equivalent to the size of the whole particles into the outer cylinder such this spherical geometry is completely filled up with fraction particles.

vi) Under the analyst tab in EDEM, export the position (X,Y,Z) and volume date of the fraction particles filling up the spherical geometry. Based on the coordinates and size obtained from this data, the custom factory creates fraction particles such that they form a spherical shaped cluster.

4.2.3.3 Development of Particle Replacement Factory

The *particle replacement* factory is a custom factory written in the computer language C++ included in EDEM. The purpose of this factory is to create a *dummy* particle of certain properties and replace this with a new particle of completely different properties. For the purpose of this simulation, the whole particles were replaced by the cluster of fraction particles (Figure 4-4). The replacement of the particles occurs at a defined time. At the defined time, the original whole particle is removed from the simulation and replaced by the cluster of fraction particles.

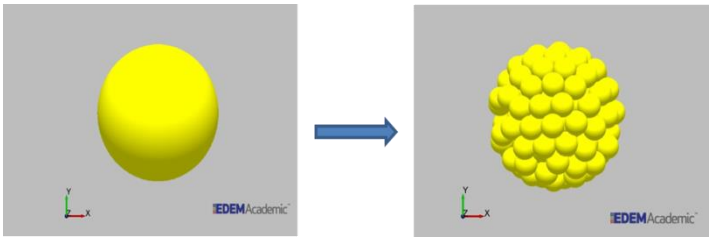

Figure 4-4: Replacement of whole particle by cluster of fraction particle using *particle replacement* factory.

4.2.3.4 Defining Particle Bonding and Breakage

After defining the whole and fraction particles and developing the custom factory to create the cluster of fraction particles, the next step is to keep this cluster of particles intact. This was done by bonding the particles. To introduce bonds between the particles, the Hertz-Mindlin with bonding contact model was used, which is based on the bonded particle model (BPM) approach developed by Potyondy and Cundall (2004). This build-in model in EDEM includes the working principles of the Hertz-Mindlin no slip contact model with the addition of the principles of the BPM. The advantage of using the Hertz-Mindlin with bonding contact model is that before bond formation and after bond breakage, the particle behavior and interaction is based on the Hertz-Mindlin with no-slip contact model and when the bonds are formed between particles, the

particle-bond systems interact according to the BPM. Figure 4-5 depicts the working principle of BPM.

When two particles come in contact, overlapping takes place between these particles as a representation of the deformation taking place due to the contact. Depending on the extent of the overlap region between these particles, a parallel bond is formed at the center of this overlap region as shown in the Figure 4-5. However, the bond creation also depends on certain defined parameters of the BPM, given in Table 4-3. Out of the parameters given in the table, creation of the bond between the particles primarily depends on the bond start time, and the bond radius. The bond start time is the time at which the model creates bonds between all particles in contact. This time can be manually selected to suit the needs of the process being modeled. For this study, a bond start time of 0.29s was selected which is the time when the whole particles were replaced by the cluster of fraction particle using the particle replacement factory and in the immediate next time step, bonding was introduced between the particles of the cluster to retain the spherical shape of the cluster. At this particular time, a bond is formed between all of those particles contacting other particles provided the extent of this overlap falls within a certain radius referred to as the bond radius. The strength of this parallel bond formed between the particles depends on the shear stress and stiffness values (Table 4-3).

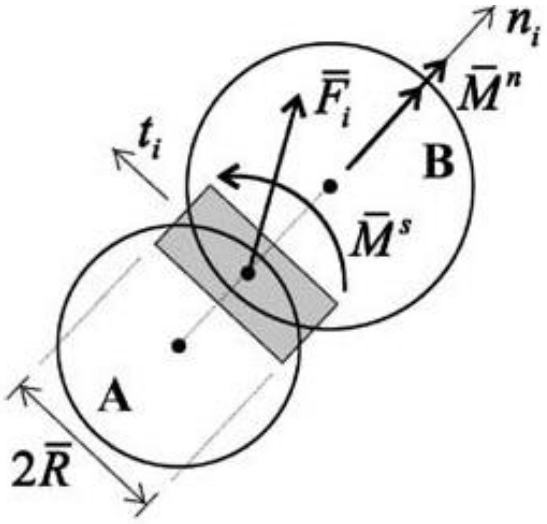

Figure 4-5: Force-displacement behavior of particle bond system

The bond between each particle is modeled as a set of elastic springs distributed over a circular cross section which transfers the translational and rotational motion experienced by one particle to the other particle it is bonded to (Metzger & Glasser, 2012). Once the particles are bonded, the forces and moments acting on the bonds are calculated by the model. These are given by the following equations.

$$\Delta\bar{F}^n = \bar{k}^n A \Delta U^n \quad \textbf{4-1}$$

$$\Delta\bar{F}^s = -\bar{k}^s A \Delta U^s \quad \textbf{4-2}$$

$$\Delta\bar{M}^n = -\bar{k}^s J \Delta\theta^n \quad \textbf{4-3}$$

$$\Delta\bar{M}^s = -\bar{k}^n I \Delta\theta^s \quad \textbf{4-4}$$

Similarly, the maximum force the bond withstands is predetermined using the following equations. A force exceeding this pre-set critical stress values results in the breakage of the bonds.

$$\bar{\sigma}_{max} = \frac{-\bar{F}^n}{A} + \frac{|\bar{M}^s|\bar{R}}{I} < \bar{\sigma}_c \quad \textbf{4-5}$$

$$\bar{\tau}_{max} = \frac{|\bar{F}^s|}{A} + \frac{|\bar{M}^n|\bar{R}}{J} < \bar{\tau}_c \quad \textbf{4-6}$$

where, $\bar{F}^n$, $\bar{F}^s$, $\bar{M}^n$, $\bar{M}^s$ denote the axial – and shear – directed force and moments respectively; U^n, U^s, θ^n, θ^s denote the relative displacement – and rotation component in the axial and shear directions; *A, I, J* are the area, moment of inertia and the polar moment of inertia of the parallel bond; $\bar{\sigma}_{max}$, $\bar{\sigma}_c$, $\bar{\tau}_{max}$, $\bar{\tau}_c$ denote the maximum and critical tensile stress and shear stress cutoff values the bond can withstand; and $\bar{R}$ denotes the parallel bond radius. If any of the critical values is exceeded, the bond breaks.

To apply the BPM, the assumptions in this single sphere approach model development are: i) the bran and flour particles are uniform in size and shape; ii) the endosperm is comprised of flour and bran particles that are clustered with same bond strength; iii) bond strength is uniform within any part of the kernel;

Table 4-2: Property input values used for particles and rolls

Moisture content, % w.b.	Particle radius*, μm	Particle density, kg/m^3	Poissons ratio	Shear modulus, MPa	Coefficient of restitution	Coefficient of static friction	Coefficient of rolling friction
Wheat kernel							
12.00	1275.00 (200.00)	1423.00	0.20	76.50	0.33	0.38	0.19
14.00	1295.00 (200.00)	1420.00	0.20	76.50	0.32	0.39	0.19
16.00	1305.00 (205.00)	1416.00	0.20	76.50	0.32	0.40	0.20
1st break stream							
12.00	282.79	1453.00	0.20	76.50	0.27	0.33	0.17
14.00	295.55	1450.00	0.20	76.50	0.30	0.36	0.18
16.00	400.21	1431.00	0.20	76.50	0.31	0.37	0.23
Roll stand, steel							
	-	7800.00	0.30	77000.00	-	-	-

*The values in parenthesis indicate the standard deviation given to the particle radius.

Note: The standard deviation was given as input only for the particle radius of wheat kernels. For all other properties only mean values were used.

Table 4-3: Simulation inputs for bonded particle model

Bond parameters	Critical value
Normal stiffness*, N/m^3	1×10^8
Shear stiffness*, N/m^3	1×10^8
Normal stress*, Pa	1.275×10^7
Shear stress*, Pa	1.275×10^7
Bond radius, mm	1
Bond start time, s	0.29

*Values from Morris et al., 2008;

4.2.4 Single Sphere Approach Model Validation

Samples of HRW wheat were collected from the Hal Ross Flour Mill at Kansas State University. The moisture content of the samples was determined using the AOAC standard procedure 925.10 (AOAC, 2000) by drying 2 to 3g of the sample in a hot air oven at 130°C for 60 minutes. The moisture content of the samples was adjusted to 12%, 14% and 16% (wet basis) by adding the proper moisture for the required adjustments based on dry matter content (Kingsly & Ileleji, 2009).

Milling trials of the collected wheat samples (conditioned to12, 14, and 16% moisture content, wet basis) were conducted on the Ross Tabletop experimental roller mill (Ross, OK, USA) in the milling lab at the Department of Grain Science and Industry, Kansas State University, Manhattan, KS. The wheat was milled through the 1st break rolls. The roll specifications were adjusted to a speed differential of 2.5:1 with a 1st break release of 28-32%. Three milling trials of 1000g wheat per trial at each moisture level were performed. The break release for each trial was determined using the % mass of ground wheat passing through the 1041µm (US 20SSBC) sieve opening when sifted for 2 mins in a Great Western Lab Sifter (Great Western Co., KS, USA) with a sieve stack of 20SSBC (1041 µm), 50GG (375 µm), 70GG (240 µm), 10XX (132 µm) and a pan (Pasikatan, 2000). The roll gap corresponding to this break release was 6.35mm. The particle size and size distribution of the 1st break collected post milling was determined for each of the 1st break samples using the ASABE standard S319.4 (ASABE,

2000) by sifting the material for 15 mins with a stack of 3 sieves 20 SSBC (1041 µm), 24SSBC (869µm), 10XX (132µm) and pan.

To perform additional validation studies, samples of HRW wheat and 1st break were collected from the pilot-scale Hal Ross Flour Mill and the mean particle size and size distribution of these 1st break samples was calculated using the ASABE standard S319.4 (ASABE, 2000) technique as mentioned above. The above samples collected were at a moisture content of 16% (wet basis). And the break release maintained at the Hal Ross Flour Mill for HRW wheat milling was 33%. The mean geometric particle size and size distribution of these samples was compared with the model results.

The mean relative percent deviation of the particle size and size distribution obtained from the model and the milling trials was determined using the following formula:

$$P = \frac{100}{N} \times \sum \frac{|Y - Y_p|}{Y} \qquad \textbf{4-7}$$

where Y is the experimental value; Y_p is the predicted value; and N is the number of observations, or the number of sieve openings which were used to calculate the mean geometric particle size.

4.2.5 Sensitivity Analysis

Sensitivity analysis for the model was carried out by varying the shear modulus and coefficient of restitution property values. The purpose of performing a sensitivity analysis was to decrease the mean relative percent deviation of the model and also to determine the influence of parameter values on the overall size and size distribution of 1st break stream. The rationale behind the selection of these parameters was due to the limited availability in literature of these property values for 1st break stream samples.

A wide range of values have been published for the elasticity modulus of wheat (Moya et al., 2002; Markauskas et al., 2010; Figueroa et al., 2011; Khodabakshian & Emadi, 2011; Weigler et al., 2012; Moya et al., 2013; Sarnavi et al., 2013) and the elasticity modulus of endosperm (Haddad et al., 1998; Haddad et al., 1999; Delwiche, 2000; Morris et al., 2008) determined on the basis of different techniques. The relationship between shear modulus and elasticity modulus is:

$$E = 2G(1 + v) \qquad \textbf{4-8}$$

where G is the shear modulus; E is the elasticity or Young's modulus; and v is the Poisson's ratio.

A wide range of shear modulus values from 0.53 to 76.5 MPa was obtained for wheat kernels and the endosperm using equation 4-8. Such a wide variation in the shear modulus values was observed primarily due to the difference in the techniques used to determine the elasticity modulus of the grains and endosperms. In certain studies, whole grains were used for measurement while in others, bulk grains were used. Khodabakshian & Emadi, (2011) have provided a list of the different studies conducted and the techniques and theories used for each of these studies.

Due to the non-availability of literature values on the shear modulus of 1st break stream, values ranging from 0.53 to 76.5 MPa were used for sensitivity analysis. This range encompasses the shear modulus of wheat kernels and endosperm.

Prior to performing sensitivity analysis, the model used the properties given in Table 4-2. The shear modulus value used as inputs for the 1st break in this model was 76.5 MPa. Sensitivity analysis was performed in two stages. First, the milling process was simulated by changing the shear modulus values. But since EDEM takes in account only 1 significant digit, the shear modulus values used ranged from 1 to 76.5 MPa. These values were used in increments of 10 MPa i.e. starting from 1, 10, 20, 30, 40, 50, 60, 70 and 76.5 MPa. The resulting mean geometric particle size and size distribution obtained from each of these simulations was compared to the lab-scale milling results of HRW wheat at 16% moisture content (wet basis) until the closest distribution to the lab-scale milling results with least mean relative percent deviation was attained.

The coefficient of restitution value used for the original simulation, before performing sensitivity analysis with the model was 0.3, which is referred to as the base value. In the second step, the coefficient of restitution was decreased starting from 0.30 in decrements of 0.05 (i.e. 0.30, 0.25, 0.2, 0.15, 0.1, 0.05, and 0.01) until a particle size and size distribution with the least mean relative percent deviation when compared to the lab-scale milling was attained.

4.3 Results and Discussions

The primary purpose of the model was to simulate the size reduction of wheat kernels into the first break stream. As a trial, a simulation of 50 whole wheat kernels was performed. The 50 particles were fed from the hopper to the rolls as they were generated by the particle factory as shown in the Figure 4-6.

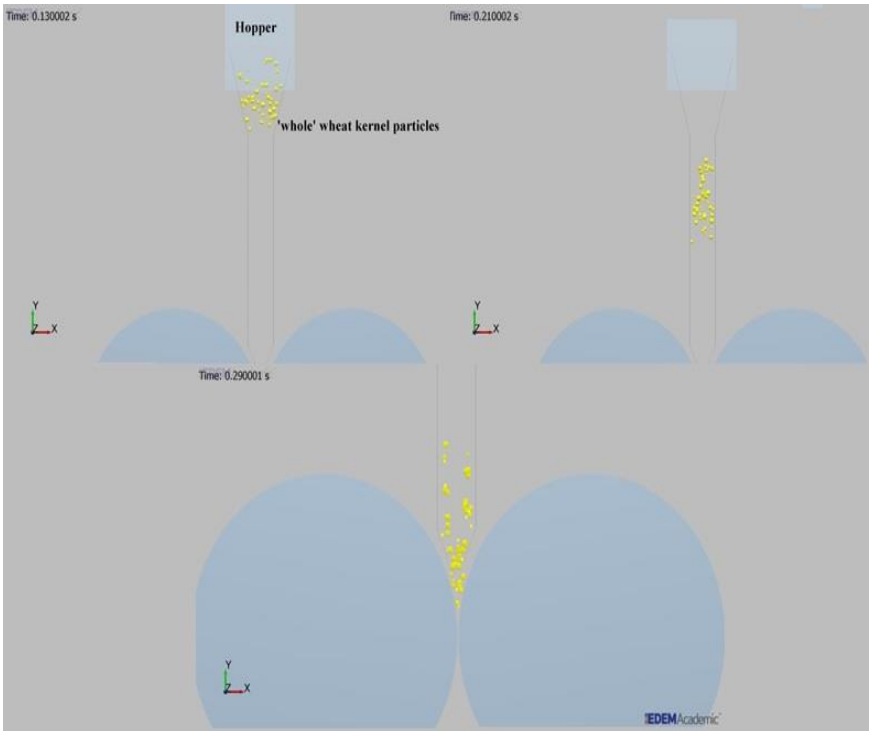

Figure 4-6: Flow of wheat kernels from hopper into break rolls

The trial simulations were run mainly to determine the functioning of the model. These simulations were run for a total simulation time of 1s which was sufficient to model the 1st break milling of the whole particles. The main intention behind simulating the process for 50 particles was to monitor if the external *particle replacement* factory and the BPM functioned together in EDEM. Some of the aspects of the model that were identified by simulating these trial simulation were: if the whole particles were being replaced by the cluster of fraction particles; if the cluster bonded together at the specified *bond start time* or not; after formation of the bonded cluster, if the breakage or size reduction was taking place when the cluster came in contact with both break roll or were the clusters breaking up even before coming in contact with the break rolls.

Obstacles identified during the preliminary simulations were corrected to ensure correct functioning of the model.

After making improvements to the 50 particle model, the milling process was simulated for 1000 wheat kernels (Figure 4-7 and Figure 4-8). The total simulation time was 1s, which took an average of 72.4 hours to model milling of 1000 kernels. The progress of the simulation was monitored to ensure the particle cluster breakage took place only as the cluster came in contact with both break rolls. The particle cluster breakage resulted due to the breakage of the bonds between the particles. The bonds between particles were given definite strength properties (Table 4-3), namely the normal and shear stress and stiffness. As the bonded cluster came in contact with the break rolls, increased compressive forces act on the particle-bond system. When the resulting compressive force of the break rolls exceeds the critical stress or stiffness value, the bond between the particles begin to break. Figure 4-11 shows the breakage of the bonded cluster as it passes through the break rolls in progressive time steps. As can be seen in Figure 4-9, as the cluster comes in contact with the break rolls, the cluster is compressed due to the compressive forces of the break rolls upon the cluster. With rotation of the rolls, flutes scrape against the cluster and break the particle-bond system due to the shear forces of the flutes as seen in Figure 4-10. This simulates the actual wheat milling process.

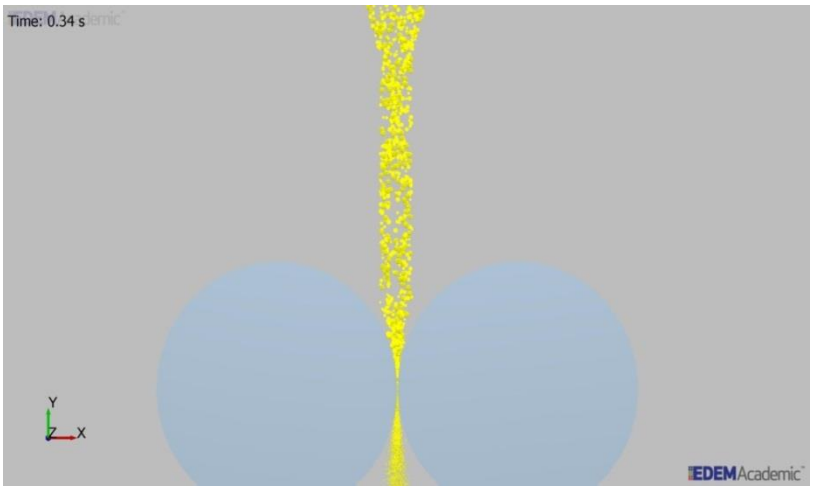

Figure 4-7: Flow of particle clusters into 1st break rolls

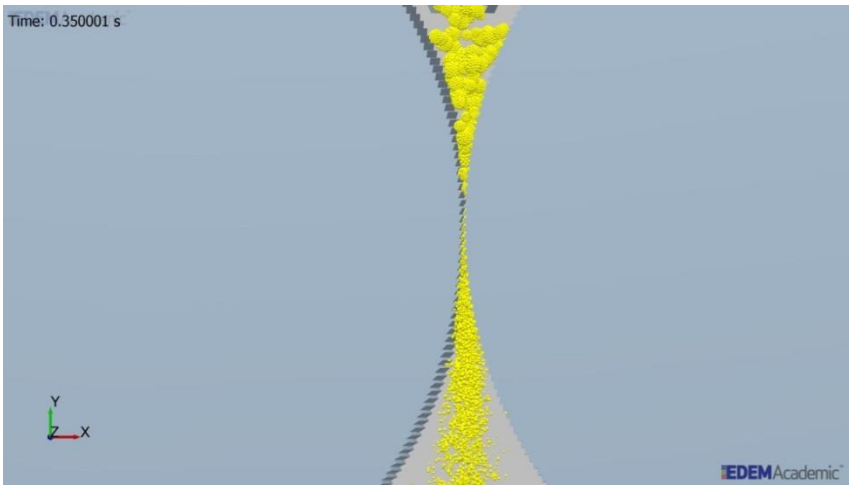

Figure 4-8: Wheat milling process – flow of clusters and breakage

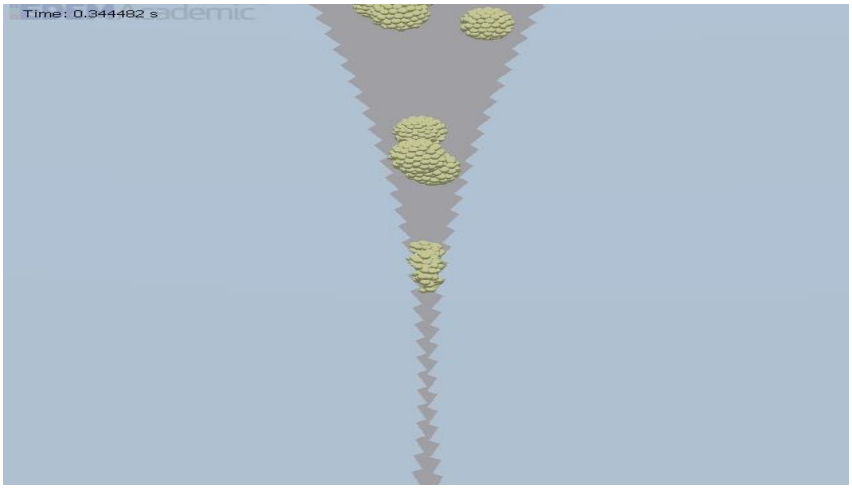

Figure 4-9: Breakage of particle cluster by compressive forces

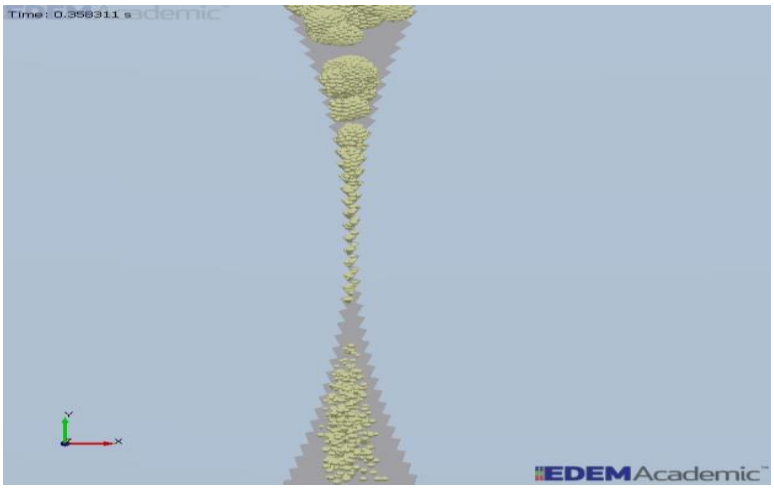

Figure 4-10: Complete breakage of particle cluster

The mass and volume of the individual whole and fraction particles at each time step of the simulation was exported from the EDEM software into a Microsoft Excel spreadsheet (Microsoft Corporation, WA, US). From the volume data of the individual particles, the time-step was selected at which all the clusters had passed through the brake rolls breaking up into the individual fraction particles. From the volume data of the fraction particles at this particular time step, the diameter of each particle was calculated and the mean particle size and size distribution of the particles was determined using the ASABE Standard S319.4 (ASABE, 2008) for calculating the mean geometric particle size. Since the bonded clusters were comprised of individual uniform spherical particles, it was assumed that these clusters break into individual particles. The size and size distribution of the particles after passage through the break rolls, was plotted as a cumulative distribution of the percent mass of sample collected at three sieves i.e. 20SSBC (1041μm), 24SSBC (869μm), 10XX (132μm), and the pan. This distribution was then compared to the cumulative distribution obtained from the lab-scale milling validation as well as the plant-scale validation trials (Figure 4-11).

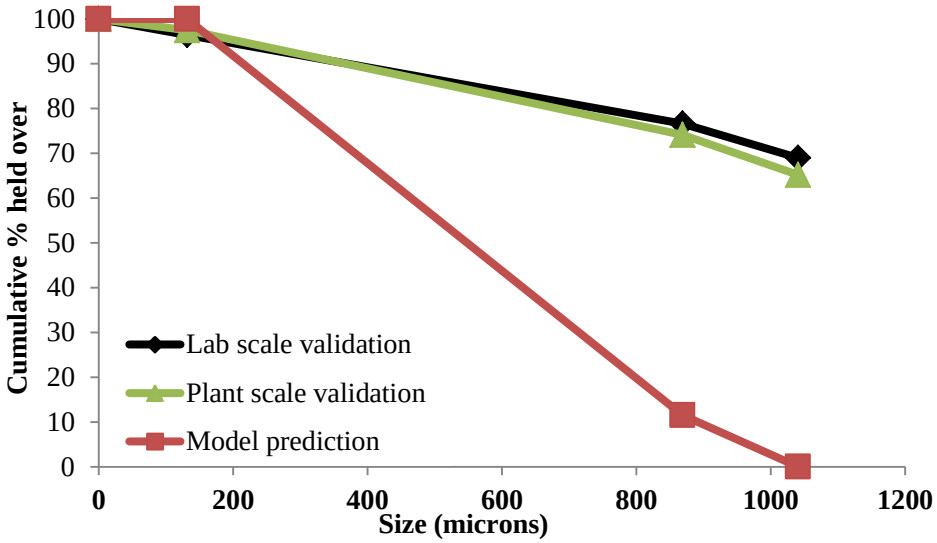

Figure 4-11: Comparison of cumulative size distribution of 1st break stream of wheat milled at 16% moisture content

The mean geometric diameter of the particles obtained from the model was 438 μm. while that from lab scale milling it was 751 μm with a mean relative percent deviation of 235%. On closer observation of the model results, it was found that there were no particles larger than 1041μm or smaller than 132μm. All particles were within the 132 - 869μm range. The model predictions had 24.84% particles with a diameter greater than 869μm and the rest of the particles were greater than 132μm. On the contrary, the lab scale milling produced approximately 69% of overs at 1041μm and 4% of 1st break flour passing through 132μm sieve opening operating at a break release of 31%. Due to the large difference in the particles collected at 1041μm and 132μm sieve openings, a high mean relative percent deviation from the model results was observed. The difference in observations between the model and lab milling could be attributed to two reasons. First, spherical agglomerates made up of uniformly sized spherical particles to represent the wheat kernel were used in the model. As size reduction takes place, the agglomerate breaks into the individual spheres or agglomerates representing flour, bran, and endosperm. However in the wheat milling process, the kernel does not break into chunks of uniformly sized particles. Instead, due to the compression and shear, the kernels break opens separating the bran, endosperm and some amount of flour resulting in a wide size distribution. Further the shapes of particles comprising the stream are not spherical. Due to the difference in shape and the size of

the particles from the model and the milling trial, this variation is observed and this is one reason that model simulations did not result in particles smaller than 132μm and bigger than 1041μm. The second reason for this observation is that in the model, uniform bond strength, represented by bond stress and shear values, throughout the bonded cluster of particle agglomerate was assumed. Due to this assumption, the kernel had a uniform hardness. But in reality, the hardness of the wheat kernel varies from the bran to germ to endosperm. As a result of these two issues, the deviation of the predictions was high.

Additional, validation of the model was performed by collecting samples of the 1st break stream from the Hal Ross flour mill and comparing the particle size and size distribution of the collected sample to the model results (Figure 4-11). The overall cumulative size distribution of the 1st break samples was quite similar to that obtained from the milling trial studies. When compared to the model, there was a significant difference in the amount of material held over the 869μm and 1041μm sieve openings with a percent relative deviation of 200%.

4.3.1 Sensitivity Analysis of the Model

A sensitivity analysis was performed to study the effect of two model parameters (shear modulus and coefficient of restitution) on the prediction of size and size distribution of the 1st break stream. The shear value used as an input in the single sphere model simulations prior to performing sensitivity analysis was 76.5 MPa for the shear modulus and 0.31 for the coefficient of restitution respectively which will be referred to as the base value. The shear modulus values for wheat kernels, reported in literature, ranged from 0.53 to 76.5 MPa.

Sensitivity analysis was performed by increasing the shear modulus in increments of 10 MPa starting with 1 MPa i.e. 1, 10, 20, 30, 40, 50, 60, 70 MPa and finally 76.5 MPa which is the highest reported value for wheat. However, it was found that the minimum value of shear modulus at which the model could simulate the milling process was 10 MPa. Consequently, for simulations with a shear modulus of 40 MPa and lower, it was found that the particle bonds began to break before the particles came in contact with the break rolls (Figures 4-12 and 4-13). It was observed that the particle-bond system began to break when the clusters came in contact with other clusters and also in contact with the walls of the feeder as shown in the Figures 4-12 and 4-13. Table 4-4 lists the mean particle size corresponding to the shear modulus values starting at 50 MPa with a maximum of 76.5 MPa. With increasing shear modulus values, the

mean geometric particle size increased. However, the increase in particle size increased the mean relative percent deviation of the predictions. Though the shear modulus value of 50 MPa resulted in low mean relative percent deviation, it also predicted the least mean geometric particle size of 1st break when compared to the lab scale validation trial results. The simulation results for shear modulus of 60 MPa and 70 MPa gave a closer mean geometric particle even though the percent deviation was on the higher side. So, the average shear modulus value of 65 MPa was selected and the model was simulated at this value. It was observed that even though the mean particle size was comparatively lower at 65 MPa than that obtained at 60 MPa and 70 MPa, the percent deviation from the different from that of the lab scale milling trials was lower which is why the shear modulus of 65 MPa was selected.

Table 4-4: Sensitivity analysis on single sphere model

Shear modulus (MPa)	**Mean geometric particle size (μm)**	**Mean relative percent deviation***
	DEM model	
50.00	368.11 (104.89)	189.87
60.00	422.58 (184.46)	226.12
65.00	371.52 (111.17)	192.29
70.00	435.35 (199.21)	233.94
76.50	437.73 (201.85)	235.37
Coefficient of restitution with a shear modulus of 65MPa		
0.25	381.60 (128.26)	199.32
0.30	374.68 (131.77)	194.55
0.31	371.52 (111.17)	192.29

* Deviation from the particle size of 751 (±511) obtained through lab scale milling trials.

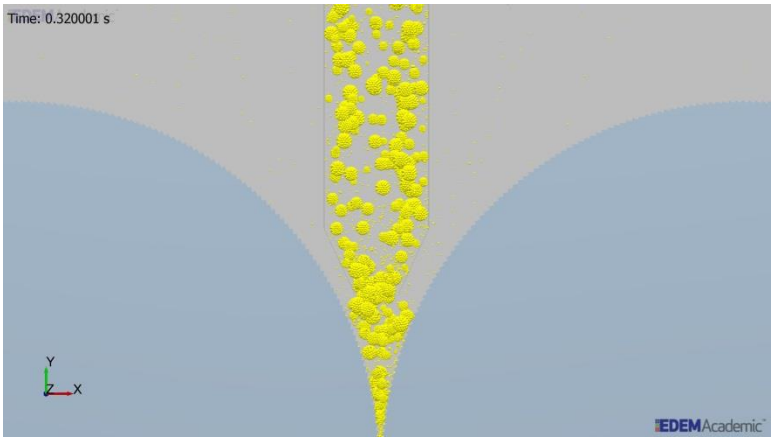

Figure 4-12: Breakage of particle-bond system in clusters at shear modulus of 40MPa

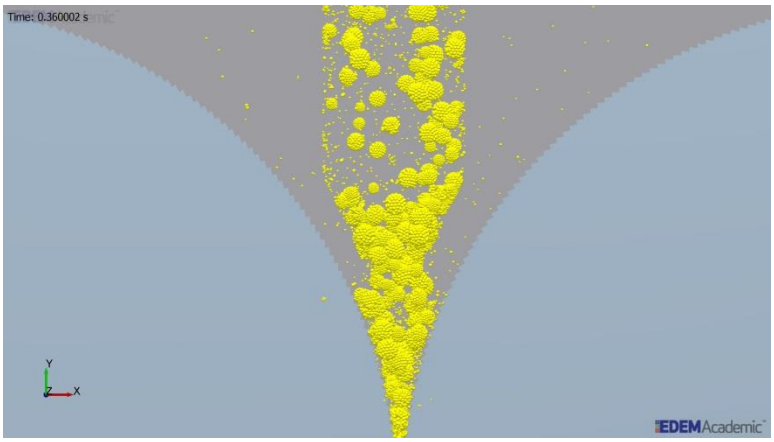

Figure 4-13: Breakage of particle-bond system in cluster at shear modulus of 30MPa

The coefficient of restitution (COR) used for simulations prior to sensitivity analysis was 0.31. After fixing the shear modulus value at 65 MPa, the COR was decreased starting from 0.3 in decrements of 0.05 i.e. 0.31, 0.3, 0.25, 0.20, 0.15, 0.10, 0.05, 0.01. Similar to the observations made for model simulations with shear modulus values of 40 MPa and lower, for COR values below 0.2 the particle bonds of the cluster did not hold until they came in contact with the break rolls (Figure 4-14). As the kernels were being fed into the break rolls from the hopper, due to the particle-particle contact and contacts with the hopper geometry, the bonds began to break, which was unrealistic. The broken particles from these clusters contacted other intact clusters and contributed to their breakage as well. For a COR of 0.25, there was an increase in the mean geometric particle size even though the mean relative percent deviation increased as well. At a COR of 0.3, the particle size was similar to that obtained at 0.31.

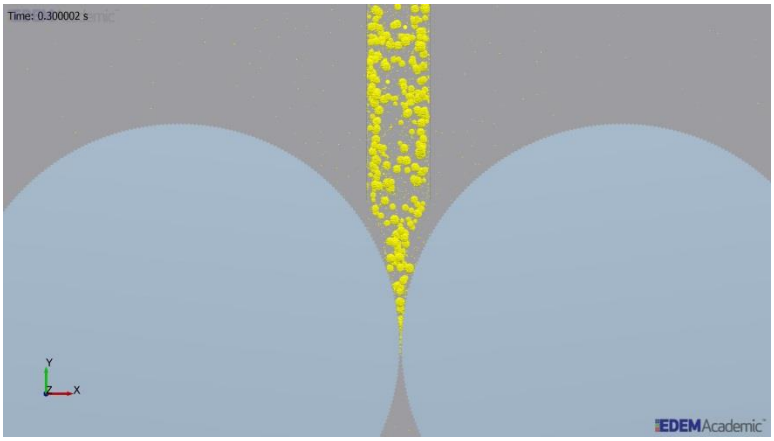

Figure 4-14: Breakage of particle-bond system in cluster at a coefficient of restitution of 0.2

Using the shear modulus and COR values of 65 MPa and 0.25, respectively, the model was was extended to simulate the milling of HRW wheat at 12 and 14% moisture content (wet basis). It was observed that with an overall increase in the moisture content, the mean particle size and size distribution of 1st break stream decreased (

Table 4-5). The same phenomenon was observed during validation trials where the mean particle size decreased with increasing wheat moisture content. But, the mean relative percent deviation was high at lower moisture contents also (Figure 4-15). The major reason behind this was the assumption that the bran, endosperm and germ making up the wheat kernel are of uniform size and shape and on passage through the 1st break rolls, the cluster of bonded 'fraction' particles representing these components breaks up into the individual particles.

Table 4-5: Change in particle size with moisture content

Moisture content, % wet basis	**Mean geometric particle size (μm)**		**Mean relative percent deviation**
	DEM model prediction	**Lab-scale validation**	
12.00	412.72 (172.32)	808.44 (488.31)	246.61 %
14.00	410.41 (169.38)	787.03 (499.86)	232.78 %

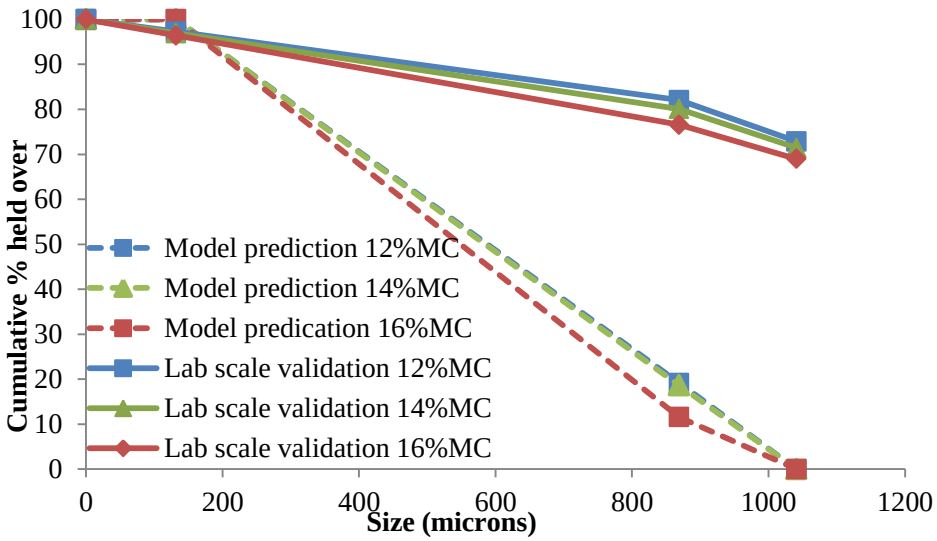

Figure 4-15: Cumulative size distribution comparison of DEM model and milling trial results at different moisture content

4.4 Conclusion

The DEM modeling technique was applied to predict the 1st break wheat milling process. The single sphere approach was used in the model development. A bonded particle model in combination with a particle replacement custom factory was used to create a bonded cluster representing the break stream. The cluster was comprised of uniformly sized spherical particles with fixed bond strength. The DEM model was able to simulate the wheat kernel breakage during the 1st break milling process. The average particle size obtained from the DEM model, for HRW wheat at 16% moisture content, was 438μm with a percent relative deviation of 235%. This was because of the use of uniformly size fraction particles to make up the wheat kernel which resulted in not taking into account the distribution in size that is observed for each of the components of the kernel i.e. the endosperm, bran, and germ individually.

Sensitivity analysis of the model was performed by varying the shear modulus and coefficient of restitution. At a shear modulus of 65 MPa and coefficient of restitution of 0.25, the mean particle size decreased to 382 μm with a percent deviation of 199%. The unrealistic assumptions in the DEM model such as bonded clusters comprised of uniformly sized particles and constant bond strength resulted in a high deviation from measured values. In wheat kernels the hardness of the kernel varies between the endosperm portion and the bran and germ portions.

The optimized model was applied to predict the 1st break milling of HRW wheat at 12 and 14% moisture content. The predicted particle size decreased with increasing moisture content as was observed during validation trials. Overall, the single sphere approach predicted the variation in the particle size and size distribution with moisture content during 1st break milling.

4.5 References

AOAC. (2000). 925.10: Solids (total) and moisture in flour – Air oven method. In *Official Methods of Analysis.* 17th ed. Gaithersburg, Md. : AOAC International.

ASABE. (2008). S 319.4: Method of determining and expressing fineness of feed materials by sieving. St. Joseph, Mich.: ASABE.

Boac, J. M., Casada, M. E., Maghirang, R. G., & Harner, J. P., III. (2010). Material and interaction properties of selected grains and oilseeds for modeling discrete particles. *Transactions of the Asabe, 53*(4), 1201-1216.

Campbell, G. M., Bunn, P. J., Webb, C., & Hook, S. C. W. (2001). On predicting roller milling performance Part II. The breakage function. *Powder Technology, 115*(3), 243-255.

Campbell, G. M., Fang, C., & Muhamad, I. I. (2007). On predicting roller milling performance VI - Effect of kernel hardness and shape on the particle size distribution from first break milling of wheat. *Food and Bioproducts Processing, 85*(C1), 7-23.

Cleary, P. W. (2001). Recent advances in DEM modeling of tumbling mills. *Minerals Engineering, 14*(10), 1295-1319.

Coetzee, C. J., Basson, A. H., & Vermeer, P. A. (2007). Discrete and continuum modelling of excavator bucket filling. *Journal of Terramechanics, 44*(2), 177-186.

Coetze, C. J., Els, D. N. J., & Dymond, G. F. (2010). Discrete element parameter calibration and the modelling of dragline bucket filling. *Journal of Terramechanics, 47*(1), 33-44.

Cundall, P. A., & Strack, O. D. L. (1979). Discrete numerical-model for granular assemblies. *Geotechnique, 29*(1), 47-65.

Delwiche, S. R. (2000). Wheat endosperm compressive strength properties as affected by moisture. *Transactions of the ASAE, 43*(2), 365-373.

Dziki, D. (2008). The crushing of wheat kernels and its consequence on the grinding process. *Powder Technology, 185*(2), 181-186.

Dziki, D., & Laskowski, J. (2004). Influence of kernel size on grinding process of wheat at respective grinding stages. *Polish Journal of Food and Nutrition Sciences, 13*(1), 29-33.

Fang, Q., Biby, G., Haque, E., Hanna, M. A., & Spillman, C. K. (1998). Neural network modeling of physical properties of ground wheat. *Cereal Chemistry, 75*(2), 251-253.

Figueroa, J. D. C., Hernandez, Z. J. E., Veles, M. J. J., Rayas-Duarte, P., Martinez-Flores, H. E., & Ponce-Gracia, N. (2011). Evaluation of degree of elasticity and other mechanical properties of wheat kernels. *Cereal Chemistry, 88*(1), 12-18.

Fistes, A., & Tanovic, G. (2006). Predicting the size and compositional distributions of wheat flour stocks following first break roller milling using the breakage matrix approach. *Journal of Food Engineering, 75*(4), 527-534.

Gonzalez-Montellano, C., Fuentes, J. M., Ayuga-Tellez, E., & Ayuga, F. (2012). Determination of the mechanical properties of maize grains and olives required for use in DEM simulations. *Journal of Food Engineering, 111*(4), 553-562.

Haddad, Y., Benet, J. C., & Abecassis, J. (1998). A rapid generl method for appraising the rheological properties of the starchy endosperm of cereal grains. *Cereal Chemistry, 75*(5), 673-676.

Haddad, Y., Mabille, F., Mermet, A., Abecassis, J., & Benet, J. C. (1999). Rheological properties of wheat endosperm with a view on grinding behavior. *Powder Technology, 105*, 89-94.

Hertz, H. (1882). On the contact of elastic body. *Journal of Pure and Applied Mathematics, 92,* 156-171.

Khodabakshian, R., & Emadi, M. (2011). Determination of the modulus of elasticity in agricutural seeds on the basis of elasticity theory. *Middle-East Journal of Scientific Research, 7*(3), 367-373.

Kingsly, A. R. P., & Ileleji, K. E. (2009). Sorption isotherm of corn distillers dried grains with solubles (DDGS) and its prediction using chemical composition. *Food Chemistry, 116*(4), 939-946.

Markauskas, D., Kacianauskas, R., Dziugys, A., & Navakas, R. (2010). Investigation of adequacy of multi-sphere approximation of elliptical particles for DEM simulations. *Granular Matter, 12*(1), 107-123. Metzger, M. J., & Glasser, B. J. (2012). Numerical investigation of the breakage of bonded agglomerates during impact. *Powder Technology, 217*, 304-314. Mindlin, R. D., & Deresiewicz, H. (1953). Elastic sphere in

contact under varying oblique forces. *Journal of Applied Mechanics-Transactions of the Asme, 20*(3), 327-344.

Metzger, M. J., & Glasser, B J. (2013). Simulation of the breakage of bonded agglomerates in a ball mill. *Powder Technology, 237*, 286-302

Morris, C. F., Pitts, M J., Bettge, A. D., Pecka, K., King, G. E., & McCluskey, P. J. (2008). Compressive strength of wheat endosperm: Analysis of endosperm bricks. *Cereal Chemistry, 85*(3), 351-358.

Moya, M., Ayuga , F., Guaita, M., & Aguado, P. (2002). Mechanical properties of granular agricultural material. *Transactions of the ASAE, 45*(5), 1569-1577.

Moya, M., Aguado, P., & Ayuga, F. (2013). Mechanical properties of some granular agricultural material used in silo design. *Internatioal Agrophysics, 27*, 181-193.

O'Sullivan, C. (2011). Particle-based Discrete element modeling: geomechanics perspective. *International Journal of Geomechanics, 11*(6), 449-464.

Pasikatan, M. C. (2000). *Developement of First-Break Grinding Models and a Near-Infrared (NIR) Reflectance Technique for Estimation of First-Break Grinding Fractions as Bases of a Roll Gap Control Algorithm.* Doctor of Philosophy Dissertation, Kansas State University, KS, USA.

Pasikatan, M. C., Milliken, G. A., Steele, J. L., Haque, E., & Spillman, C. K. (2001). Modeling the energy requirements of first-break grinding. *Transactions of the Asae, 44*(6), 1737-1744.

Patwa, A., Ambrose, R. P. K., Dogan, H., & Casada, M. E. (2014). Wheat mill stream properties for discrete element method modeling. *Transactions of the Asabe, 57*(3), 891-899.

Potyondy, D. O., & Cundall, P. A. (2004). A bonded-particle model for rock. *International Journal of Rock Mechanics and Mining Sciences, 41*(8), 1329-1364.

Quist, J. (2012). *Cone crusher modelling and simulation- Developement of a virtual rock crushing environment based on the discrete element method with industrial scale experiments for validation.* Unpublished MS Thesis, Chalmers University of Technology, Goteborg, Sweden.

Sarnavi, H. J., Mohammadi, A. N., Motlagh, A. M., & Didar, A. R. (2013). DEM model of wheat grains in storage considering the effect of moisture content in direct shear test. *Research Journal of Applied Sciences, Engineering and Technology, 5*(3), 829-841.

Weigler, F., Scaar, H., & Mellmann, J. (2012). Investigation of particle and air flows in a mixed-flow dryer. *Drying Technology*, *30*(15), 1730-1741.

Chapter 5 - DEM Model of 1st Break Wheat Milling using a Multi-Sphere Approach

The preliminary results were presented at a conference, with the citation below.

Conference presentation:

Patwa, A., Ambrose, K. 2014. Discrete Element Method Modeling of 1st Break Wheat Milling Process using a Multi-Sphere Approach. ASABE 2014 Annual International Meeting, July, 2014. Montreal, Canada. (Oral)

The bonded particle model (BPM) approach in DEM has been largely used in the rock mechanic and mining industry to understand the breakage and fracture behavior of rocks (Potyondy and Cundall, 2004; Potyondy, 2007), ore particles (Ali and Bradshaw, 2010), cemented sand (Obermayr et al., 2013), etc. In most studies that involved the use of BPM, the built-in EDEM Hertz-Mindlin with bonding contact model was used because it takes into account the working principles of both BPM during bond formation and the Hertz-Mindlin with no slip contact model in the absence of bonding. A variation of the built-in Hertz-Mindlin with bonding contact model is an external plugin of the BPM that allows the user to define distributed bond strength throughout the bonded particle. However, not much literature is available on the use and application of this plugin with DEM for predicting size reduction of particulate materials.

5.1 Material and Methods

5.1.1 DEM Input properties

A multi-sphere model was developed using physical and mechanical properties of hard red winter (HRW) wheat and the 1st break stream at 12, 14, and 16%.

5.1.2 Discrete Element Method

EDEM software (v 2.6, DEM Solutions Ltd., Edinburgh, UK) was used. The simulations were carried out in an Intel Core 2 Duo processor with a 4 GB RAM and 64-bit Windows 7 professional operating system. The principle behind development of the model is similar to that discussed in Chapter 4 for the single sphere model.

5.1.2.1 Creating Particles and Custom Factory

This DEM model for the single sphere model is extended to a multi-layered particle made up of 4 spheres (Figure 5-1) with varying bond strength throughout the kernel.

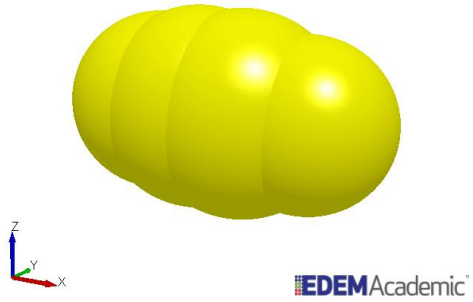

Figure 5-1: Four sphere wheat kernel particle

To develop the multi-layered particle, four spherical particles were overlapped forming a shape similar to that of a wheat kernel (Figure 5-1). A custom particle factory was created to fill the four-sphere whole particle with smaller particle fractions characterized by the properties of 1st break wheat mill stream. The procedure followed to create custom factory is given below:

i) Created two rectangular boxes around the origin in EDEM that is large enough to fit the whole wheat particle. The outer box is considered to be the container and the inner box as the particle factory that contained fraction particles (Figure 5-2).

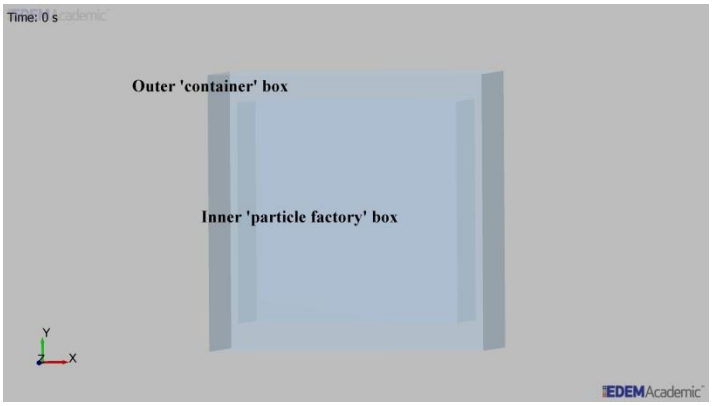

Figure 5-2: Creation of box geometries for custom factory

ii) Defined fraction particles with measured properties and radius such that the contact radius is slightly larger than the physical radius. The contact radius is an imaginary radius of the particle used by the model for the purpose of bond creation between two particles. Further explanations on the contact radii are provided in the following section.

iii) Defined the particle factory for the fraction particles by giving them a normal size distribution. Normal size distribution can be given as an input in EDEM by defining the mean and standard deviation of the particle under the factory domain in EDEM.

iv) Simulated the filling up of the container box with the fraction particles and allowed the particles to settle down at the bottom of the container (Figure 5-3).

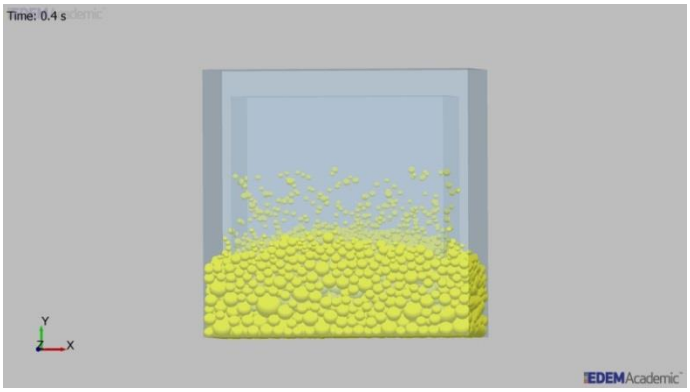

Figure 5-3: Particles being generated in the custom factory

v) Upon completion of the simulation, the geometry of the 4-sphere particle equivalent to the size of the whole particles was imported into the outer cylinder such that the 4-sphere geometry is completely filled with fraction particles (Figure 5-4).

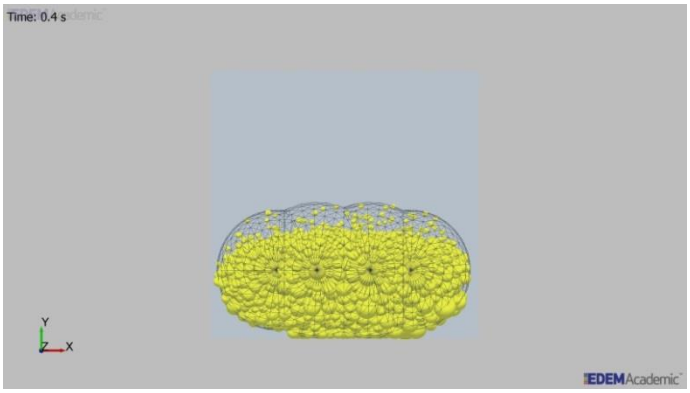

Figure 5-4: Selection of particles within the space by importing 4-sphere geometry

vi) The position (X,Y,Z) and volume date of the fraction particles filling up the spherical geometry was exported. Based on the coordinates and size obtained from this data, the custom factory created fraction particles which formed a cluster in the shape of a 4-sphered particle. It uses the X, Y, Z co-ordinates and the scaling factor of the particles. The scaling factor is a number calculated from the radius of the particles of the cluster in comparison to the mean radius given as input to the model for creation of the prototype fraction particle.

5.1.2.2 Particle Replacement Factory

Similar to the single sphere model (Chapter 4), a particle replacement factory was used to replace the whole wheat particles by the fraction particles at a defined time. In this model, the whole particle is replaced by a cluster of fraction particles similar in size and shape (Figure 5-5). This cluster comprised of fraction particles with a normal size distribution.

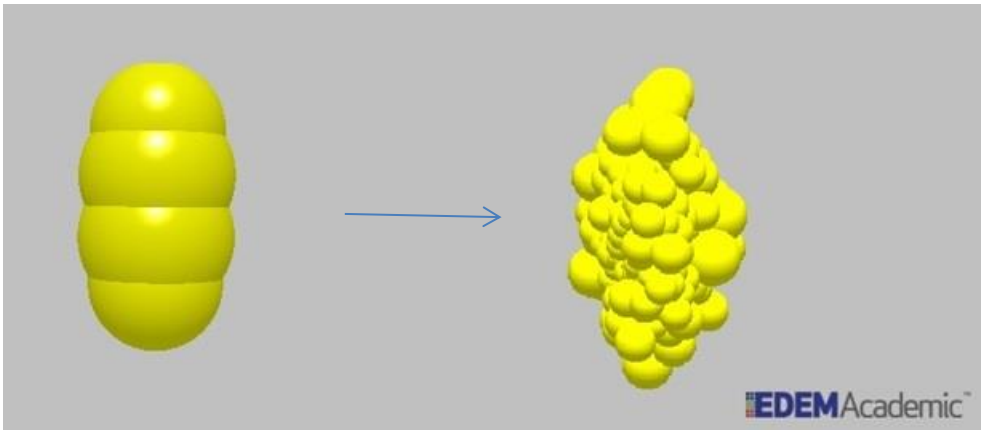

Figure 5-5: Replacement of whole particle by bonded cluster of fraction particle using *particle replacement* factory

5.1.2.3 Particle Bonding

In this 4-sphere approach, particle bonds were introduced to create a cluster of bonded particles rather than a uniform bond approach as used in Chapter 4. Instead of using the EDEM's built-in Hertz-Mindlin with Bonding contact model, an external user-defined plugin of this model was used which had been written in the computer programming language C++ by the EDEM support team. The working principle of both approaches was the same. But, the difference in the external plugin is that the bond strength parameters can be given a range a

values giving the particle-bond system making up the bonded particles a varied bond strength instead of a fixed value. The bond strength distribution defined for the cluster of 'fractions' ranged from 8.75×10^7 to 1.1275×10^8 N/m^2 which was given as input to the normal and shear stiffness with a critical normal and shear stress of 1.275×10^7 Pa. This range of bond stiffness values was selected based on the resulted reported from the work done by Morris et al., 2008 and Sarnavi et al., 2013. This enabled the use of evenly varying and distributed bond strength throughout the particle cluster. The distribution of bond strength value to the bonds formed between the particles is governed by the model which randomly distributed the bond strength depending on the number of bonds being formed for each particle.

The purpose of bond strength distribution was to create a cluster of bonded particles with varying bond strength. The hardness of a wheat kernel is not uniform but varies from the bran to the endosperm due to their difference in composition and structural build. The model randomly assigned bond strength, within the selected range, such that the strength is evenly distributed throughout the particle cluster. In addition to the bond stiffness distribution, additional parameters were also defined for the bond formation between the 'fraction' particles, listed in Table 5-1.

Table 5-1: Input parameters for bonded particle model plugin

Bond parameters	Value
Bond formation time, s	0.29
Single sphere contact radius, %	75
Particle	Fraction
Normal stiffness*, N/m^2	1×10^8 +/- 1.275×10^7
Shear stiffness*, N/m^2	1×10^8 +/- 1.275×10^7
Critical normal stress*, Pa	1.275×10^7
Critical shear stress*, Pa	1.275×10^7
Bond disk scale	1

*From Morris et al., 2008 and Sarnavi et al., 2013.

Apart from the bond strength parameters listed in Table 5-1, other user defined parameters such as the bond formation time, single sphere contact radius and bond disc scale

were also given as inputs to the BPM plugin. In this simulation, the introduction of bonds between particles is primarily time-dependent and entirely upon the user to define the time at which the model introduced bonding between particles. The bond formation time given as an input refers to this time at which bonds are to be created by the BPM plugin between the 'fraction' particles. To suit this simulation on 1st break milling of wheat, the bond formation time was selected at a time right before the particles entered the break rolls. At this bond formation time, the model begins to create a bond between each of the particles that are in contact and overlap with other particles. However, the other parameters on which bond formation depends are the bond disc scale and the single sphere contact radius. The bond disc scale refers to the scale of the bonds in terms of the particle radius i.e. the length of the bond created between two particles depending on the radius of the individual particles. The single sphere contact radius is the radius of the individual particles in contact, different from the physical radius. The contact radius is the imaginary radius used by the model to determine the area in which the particle bond can be formed. At the time of particle bonding, if the contact radii of the particles overlap, then bond formation occurs (Figure 5-6). To facilitate bond formation between two particles, a contact radius larger than the physical radius of the particle by a percentage is used. At the time of particle creation in EDEM, instead of using the same contact and physical radius, a different value is defined for the particle. Similarly, the BPM plugin also has the contact radius parameter defined. In this simulation the defined contact radius was 75% times the physical radius of the particle so that the entire particle cluster could be bonded. Since the physical radius of the 'fraction' particles was 0.4 mm, the contact radius used was 0.7 mm.

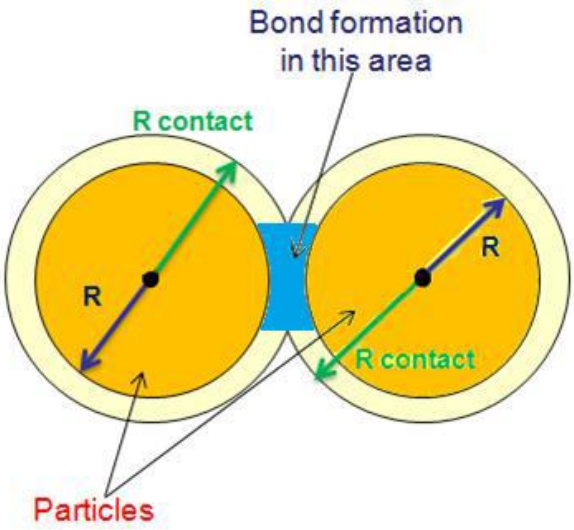

Figure 5-6: Contact radius and bond formation in BPM (EDEM, 2013)

5.1.3 Multi Sphere Model Validation

The validation of the multi sphere model was performed using the wheat milling data obtained through lab scale and pilot scale milling trials. Lab scale milling was conducted on the Ross Tabletop experimental roller mill (Ross, OK, USA) in the milling lab at the Department of Grain Science and Industry, Kansas State University, Manhattan, KS. Samples for lab scale validation were collected from the Hal Ross Mill. Moisture content of these samples was determined using the AOAC standard procedure 925.10 (AOAC, 2000) by drying 2 to 3g sample in a hot air oven at 130°C for 60 minutes. For the purpose of lab scale validation, moisture content of the wheat samples was adjusted to 12, 14, and 16% (wet basis) based on their dry matter content as per Kingsly & Ileleji (2009). Pilot scale validation was performed at the Hal Ross Flour Mill, Kansas State University. Samples before and after milling in the pilot plant were collected and their moisture content was determined. The particle size and size distribution of HRW wheat and 1st break stream obtained from lab scale milling and plant scale milling were measured using the ASABE Standard S319.4 (ASABE, 2000).

In lab-scale milling, the 1st break roll specifications were adjusted to a speed differential of 2.5:1 with a 1st break release of 28-32%. The roll gap corresponding to this break release was 6.35mm.Three milling trials with 1000g wheat per trial at each moisture level were performed. The break release for each trial was determined using the % mass of ground wheat passing

through the 1041µm (US 20SSBC) sieve opening when sifted for 2 min in a Great Western Lab Sifter (Great Western Co., KS, USA). The sifter contained a sieve stack of 20SSBC (1041 µm), 50GG (375 µm), 70GG (240 µm), 10XX (132 µm), and a pan (Pasikatan, 2000). The particle size and size distribution of the 1st break collected post milling was determined by sifting the material for 15 min based on the ASABE standard S319.4 (ASABE, 2000) with a stack of 3 sieves 20 SSBC (1041 µm), 24SSBC (869µm), 10XX (132µm), and pan.

The mean relative percent deviation of the particle size and size distribution obtained from the model and the milling trials was determined using the following formula:

$$P = \frac{100}{N} \times \sum \frac{\left|Y - Y_p\right|}{Y} \qquad \textbf{5-1}$$

where Y is the experimental value; Y_p is the predicted value; and N is the number of observations, or the number of sieve openings which were used to calculate the mean geometric particle size.

5.2 Results and Discussions

The aim of this work was to simulate the 1st break milling process of wheat by approximating the shape of whole particles similar to that of wheat kernels using multi-layered spheres (Figure 5-1). In addition varying bond strength to depict the varying strength between the endosperm and bran layer was used in this approach. The model was run for a total simulation time of 1s which took an average 200.6 h for completion. Since a normal distribution was given to the cluster of fraction particles making up the whole particles using the custom factory, each whole particle was replaced by a cluster of 971 fraction particles that were bonded together. Upon completion of the simulations, the mass and volume data for all particles at each time step of the simulation was exported into a Microsoft Excel spreadsheet (Microsoft Corporation, WA, USA) from the EDEM analyst tab and the diameter of the particles were determined. The particular time step at which all particles pass through the break roll was selected to calculate the mean geometric particle size and size distribution of the clusters after milling.

The model predicted a mean geometric particle size of 413 µm for HRW wheat milled at 16% moisture content. Figure 5-7 shows a cumulative distribution comparison of the results obtained from the model prediction, lab scale validation and pilot scale validation trials at 16%

moisture level. There was also a considerable difference in the mean particle size predicted by the model when compared to the pilot scale and lab scale validation trials Table 5-2.

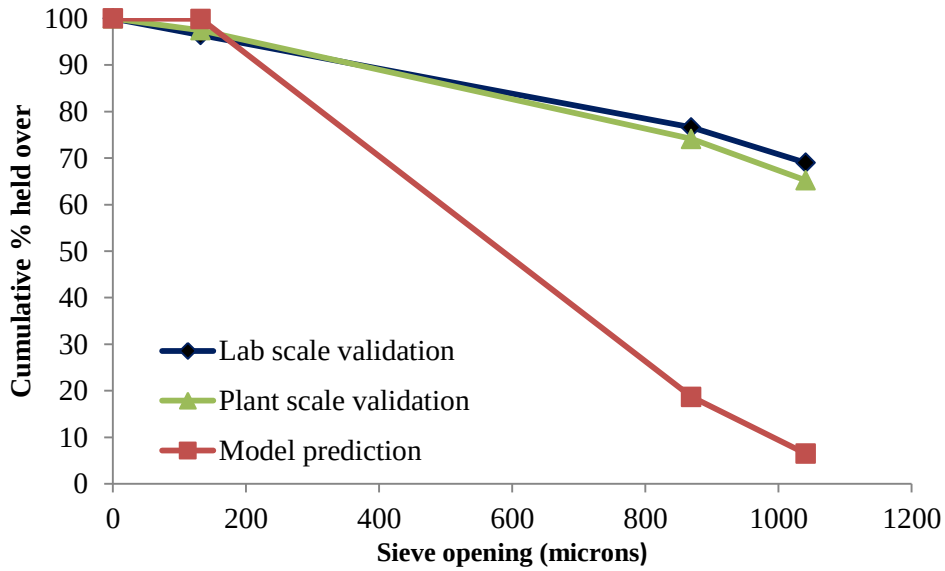

Figure 5-7: Cumulative particle size distribution of 1st break stream

Table 5-2: Particle size comparison when milled at 16% moisture content

Validation technique	Mean geometric particle size (µm)	Percent relative deviation*
DEM model prediction	412.65 (178.02)	-
Lab scale milling	751.21 (511.18)	185.89
Pilot scale milling	742.17 (476.04)	156.78

* Deviation from DEM model prediction.

A high percent deviation was obtained on comparison of model predictions with milling trials. The reason for this high deviation being that the model had a majority of the particles in the 132 to 869 µm range. The custom factory of 1st break fraction particles created to make the cluster comprised of particles with diameters ranging from 47 to 1387 µm. However, as the clusters came in contact with the break rolls, it resulted in the breakage of the cluster into the individual fraction particles resulting in a majority of the particle within the 132 to 869 µm range. A better understanding of the breakage of the clusters can be made from the series of

images (Figure 5-8 – Figure 5-10) presented here taken during the progress of the simulation. From these images, it can be observed that as the cluster comes in contact with the break rolls, forces from the rolls act on the clusters, which results in their breakage. The magnitude of these forces is such that it exceeds the bond strength of the particle-bond system. The BPM characterized the bond created between particles in such a way that if the magnitude of the force acting on the particles is greater than any of the bond strength parameters given to the model, the particle-bond system breaks which is being observed in this case. Depending on the inputs given to the model, the minimum force required to break the bond was calculated from the bond strength and contact radius values using the relation between the stress and force application. A minimum force of 6.25N acting on the clusters, which was theoretically calculated, would result in the bond breakage. It can be speculated at this point that the force acting on the bonded cluster is of compressive and shear type because these two types of forces govern the size reduction of wheat during break milling. However, no definite conclusion can be made regarding what percent of the force acting on these clusters is of the compressive type and what percent is shearing forces.

Figure 5-8: Bonded cluster passing through the rolls during milling process

Figure 5-9: Size reduction by compression and shearing

Figure 5-10: Breakage of cluster into smaller particles

From Figure 5-7, it was evident that the major difference was the amount of material collected over the 869 µm sieve opening. The DEM model, similar to the lab scale and pilot scale milling results, predicted minimal flour production during 1st break. However, the model result was nearly 50% in deviation for percent mass collected over the 869 µm sieve. This is explained by the breakage of all particle-bond systems that formed the cluster.

The high percent deviation indicated that the bond variation assumed in this four-sphere approach did not mimic the kernel structural and strength characteristics. The problem with this approach was that the model randomly distributed the bond strength. But, in a wheat kernel, this

strength is defined across the layers of bran and endosperm. So, the bond will be stronger in some sections of the cluster and a random distribution will not be the appropriate approach.

The four-sphere DEM approach of predicting 1st break milling of HRW wheat were extended to simulate the milling process at 12 and 14% moisture content levels. The results for the model prediction at these moisture levels are summarized in Table 5-3 and the cumulative size distribution comparison is given in Figure 5-11. It was observed that with increasing moisture content, the mean particle size predicted by the model increased. The lab scale milling results displayed a similar trend (Table 5-3). In commercial mills, hard wheat is generally milled at a moisture content of 15.5-17% (Butcher & Stenvert, 1973; Fang, 1995; Fang & Campbell, 2003). The purpose of adding moisture to wheat while milling is to toughen the bran (Fang & Campbell, 2003; Niernberger, 1966; Posner & Hibbs, 2005) and make it more compliant (Dziki et al., 2010) to facilitate its separation from the endosperm in whole chunks without shattering it into smaller pieces. Addition of moisture also softens the endosperm. Similarly, when wheat is milled at lower moisture levels, particularly, 12% and 14% (wet basis), the textural characteristics of the wheat kernel especially the bran and endosperm would be different from that of wheat at 16% moisture. The bran would not be as tough and resilient and neither would the endosperm be equally soft. 1st break milling at these moisture levels would still result in separation of the bran and endosperm but keeping all other parameters constant, there would be a slightly higher percentage of shattered bran and endosperm resulting in the larger particle size with narrower distribution. This is similar to what was observed in the model, where with the increase in moisture content from 12% to 16%, the mean particle size decreased.

Table 5-3: Change in particle size with moisture content

Moisture content, % wet basis	Particle size (μm)		Percent relative deviation
	DEM model prediction	Lab scale milling validation	
12.00	465.82 (241.36.)	808.44 (488.31)	184.63
14.00	456.32 (227.99)	787.03 (499.87)	210.35
16.00	412.65 (178.02)	751.21 (511.18)	185.89

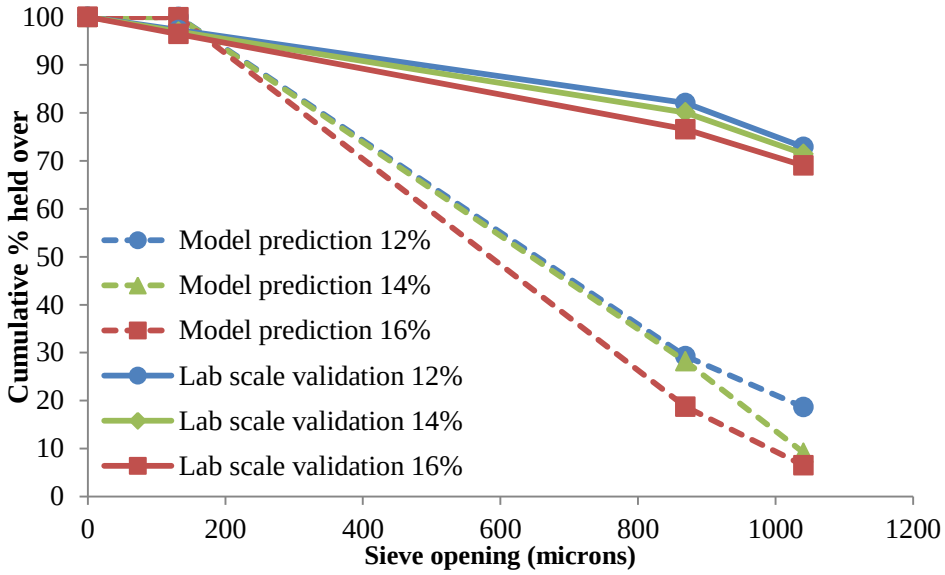

Figure 5-11: Cumulative size distribution comparison of DEM model and milling trial results at different moisture content

Even though the overall trend observed for model prediction and lab scale validation milling was similar, the percent relative deviation was considerably high. This was similar to what was observed for the comparison of the model prediction to the lab scale and pilot scale validation trials (Figure 5-7). There was a high deviation in prediction, approximately 50%, for the percent mass of ground wheat collected over the 132 µm sieve opening which was mainly due to the breakage of the cluster into individual 'fraction' particles that it was made up of.

5.3 Conclusion

A multi-layered sphere approach was used to develop a DEM model to predict the 1st break wheat milling process. Multi-spheres were used to approximate the shape of wheat kernel. The bond strength was also distributed within the wheat kernel to mimic the structural variation in a wheat kernel. The model predicted an average particle size of 413 µm for 1st break milling at 16% moisture content. The model predicted value had a percent deviation from the lab scale and pilot scale validation of 186 and 157%, respectively, which was considerably high. Because of the greater size reduction of bonded cluster the percent deviation was high. The bonded cluster created using the custom factory contained a larger number of fraction particles ranging from 132 to 869 µm. On passing through the break rolls this cluster broke into the individual fraction particles resulting in the high deviation in prediction. In addition, the model randomly assigned

the bond strength to the particle-bond system in a way that it is evenly distributed throughout the cluster within the given range. Due to this random assignment, the bond strength distribution did not correctly represent the structural characteristics of wheat kernels in terms of hardness.

The multi-sphere model was also extended to simulate the milling of HRW wheat at 12% and 14% moisture content (wet basis). With the increase in moisture content from 12% to 14%, the mean particle size decreased which was also observed at the lab scale milling trials. In conclusion, the model predicted the mean particle size of ground wheat from 1st break milling. But additional work is needed to decrease the percent deviation.

5.4 References

Ali, A. Y., & Bradshaw, S. M. (2010). Bonded-particle modelling of microwave-induced damage in ore particles. *Minerals Engineering, 23*(10), 780-790.

AOAC. (2000). 925.10: Solids (total) and moisture in flour – Air oven method. In *Official Methods of Analysis*. 17th ed. Gaithersburg, Md. : AOAC International.

ASABE. (2008). S 319.4: Method of determining and expressing fineness of feed materials by sieving. St. Joseph, Mich.: ASABE.

Dziki, D., Laskowski, J., Siastala, M., & Biernacka, B. (2010). Influence of moisture content on the wheat kernel mechanical properties determined on the basis of shear test. *International Agrophysics, 24*(3), 237-242.

EDEM (2013). EDEM Tutorial: Bonded particles model simulation. DEM Solutions, Edinburgh, UK.

Fang, Q. (1995). *Effects of physical properties and wheat and operational parameters of roller mills on size reduction.* Masters, Kansas State University.

Fang, C., & Campbell, G. M. (2003). On predicting roller milling performance V: effect of moisture content on the particle size distribution from first break milling of wheat. *Journal of Cereal Science, 37*(1), 31-41.

Kingsly, A. R. P., & Ileleji, K. E. (2009). Sorption isotherm of corn distillers dried grains with solubles (DDGS) and its prediction using chemical composition. *Food Chemistry, 116*(4), 939-946.

Morris, C. F., Pitts, M J., Bettge, A. D., Pecka, K., King, G. E., & McCluskey, P. J. (2008). Compressive strength of wheat endosperm: Analysis of endosperm bricks. *Cereal Chemistry, 85*(3), 351-358.

Niernberger, F. F. (1966). *Roll Diameter and Speed - their Effects on First Break Grinding of Wheat.* Master's, Kansas State University.

Obermayr, M., Dressler, K., Vrettos, C., & Eberhand, P. (2013). A bonded-particle model for cemented sand. *Computers and Geotechnics, 49*, 299-313.

Posner, E. S., & Hibbs, A. N. (2005). *Wheat flour milling*, second edition. St. Paul, Minn.: AACC International.

Potyondy, D. O., & Cundall, P. A. (2004). A bonded-particle model for rock. *International Journal of Rock Mechanics and Mining Sciences, 41*(8), 1329-1364.

Potyondy, D. O. (2011). Simulating stress corrosion with a bonded particle model for rock. *International Journal of Rock Mechanics, 44*(1), 677-691.

Sarnavi, H. J., Mohammadi, A. N., Motlagh, A. M., & Didar, A. R. (2013). DEM model of wheat grains in storage considering the effect of moisture content in direct shear test. *Research Journal of Applied Sciences, Engineering and Technology, 5*(3), 829-841.

Chapter 6 - Summary of Conclusions and Discussion

6.1 Restatement of Research Objectives and Goals

Wheat milling is a gradual size reduction process where the wheat kernel is opened up separating the endosperm from the bran layers and germ and subsequently reducing the size of the endosperm to make flour. To maximize profit, a miller must be able to produce the highest quality flour at maximum flour extraction. However, the extraction rate of flour and its quality are directly dependent on efficiency of separation of the endosperm from the bran and germ layers during the initial break wheat milling which regulates the entire flow in a mill. To enable efficient separation of the endosperm from bran and germ layers during 1st break milling, there are different grain properties and machine operational variables that directly affect this process which have been discussed in Section 2.2 of this thesis. The effect and significance of these variables on the process have also been studied using different modeling techniques as well as milling trials. Because majority of these techniques were based on statistical models, they did not take into consideration the non-uniform characteristics of the wheat kernels. Discrete element method (DEM), uses physical and mechanical properties as input parameter, was used in this study to predict the milling behavior of wheat. The working hypothesis of this study was that the mechanical properties of wheat kernels would have a direct effect on the particle size and size distribution of 1st break.

The objective of this thesis work was to develop a discrete element method (DEM) model of the 1st break wheat milling process for hard red winter (HRW) wheat milling. The specific objectives, as stated in Chapter 1 were,

1. To determine the effect of moisture content on the physical and material properties of wheat mill streams from three different wheat classes.
2. To develop and validate a DEM model of the 1st break wheat milling using a single sphere approach.
3. To develop and validate a multi-sphere DEM model of the 1st break wheat milling with varied bond strength.

The following sections of this chapter include a discussion of the content of the previous chapters in Section 6.2, a discussion on the major findings from the study and the conclusions

drawn from them in Section 6.3.Suggestions on possible future work based on the results obtained from this study and the research questions evolved from this study has been discussed in this chapter.

6.2 Project Overview

Chapter 1 includes a discussion on the rationale behind undertaking this study, the research hypothesis, objectives and goals. Chapter 2 includes a review of literature available on the studies undertaken to determine the different factors affecting the 1st break milling process and the modeling techniques used to determine the significance and effect of these factors. A detailed discussion is provided on the effect of the different grain properties and operational variables of the roll on the 1st break milling of wheat. In addition, a section on the DEM modeling technique, its working principle, and applicability is also provided in Chapter 2.

Chapter 3 highlights the 1st research objective on determination of the effect of moisture content on the physical and mechanical properties of wheat mill streams. The procedure used for measurement of these properties namely, moisture content, particle size and size distribution, bulk density, tapped density, true density, Young's modulus, coefficients of static and rolling friction, and coefficient of restitution are described. All the properties were measured for wheat kernel, 1/2nd break stream and wheat flour of hard red winter (HRW), hard red spring (HRS) and soft red winter (SRW) wheat varieties at three levels of moisture (12, 14 and 16% (wet basis)). In addition to these properties, the single kernel hardness, size and kernel weight were also measured for the wheat kernels. For comparison purposes, the chemical compositions of all the samples were also determined. All properties were measured at three moisture levels for statistical comparison and to determine the effect of moisture content on these properties.

Chapter 4 focuses on the development of the DEM model for the 1st break wheat milling process using a single sphere approach. This chapter discusses the procedure followed to develop the DEM model by making use of the Hertz-Mindlin with bonding contact model. The physical and mechanical properties of HRW wheat and 1st break measured in Chapter 3 were used as inputs to the model to simulate the 1st break milling operation. On obtaining preliminary results, sensitivity analysis was performed on the model to improve prediction with the model validated using lab and pilot scale milling trials. Sensitivity analysis was carried out by changing the shear modulus and coefficient of restitution values and the change in percent deviation calculated. The

DEM model on 1st break milling using single-sphere approach was validated by comparing the model predicted results to lab scale milling trials conducted at 12, 14 and 16% moisture content levels.

Chapter 5 discusses the development of a DEM model using a multi-sphere approach. A multi-sphere approach was used where a muli-layered particle was created resembling the wheat kernel in structure. Apart from using a multi-sphere approach, a bond distribution was also given to the bonded cluster of particles to replicate the variation in wheat kernel hardness. The model simulations were carried out for 1st break milling of HRW wheat at 16% moisture content. The validation results obtained from the lab scale and pilot scale milling trials mentioned in Chapter 4 were used for validation of this model. Discussion on the extension of this model to simulate the 1st break milling of HRW wheat at 12 and 14% moisture content were also provided along with the validation results.

6.3 Discussion of Major Findings

The major findings from each of the objectives discussed in Chapters 3, 4 and 5 are discussed in this section.

6.3.1 Effect of Moisture Content on Properties

The objective of measuring different physical and mechanical properties of wheat mill streams was to use these as input parameters in the development of the DEM model. It was observed that moisture content had a significant effect on the physical properties (particle size, size distribution, bulk and tapped densities) than when compared to its effect on material properties (Young's modulus, coefficients rolling and static friction, and coefficient of restitution) of break stream and flour from the three wheat varieties. In case of wheat kernels, the density, Young's modulus and coefficient of restitution decreased while the coefficients of friction increased with increase in moisture content from 12 to 16% (wet basis).

6.3.2 DEM model of 1st break milling

6.3.2.1 Single Sphere Approach

The 1st break wheat milling operation was simulated using DEM based on a single-sphere approach. A spherical bonded cluster made up of smaller uniformly sized spherical particles was

used to simulate the wheat kernel. The fixed bond strength was used to bond each of the particles in the cluster.

Initial model simulations of milling HRW wheat at 16% moisture content were performed which predicted an average size of 438 µm. The model was validated by performing lab scale milling trials. The model predication had a percent deviation of 235% from the milling validation results. To reduce the percent deviation of prediction, sensitivity analysis was performed on the model by changing the input parameters of shear modulus and coefficient of restitution. At shear modulus of 65 MPa and coefficient of restitution of 0.25, the model predicted a mean particle size of 382 µm with a 199 percent relative deviation. The model prediction was extended to simulate the size reduction of HRW wheat at12and 14% moisture content. The model predicted the trend of an increasing mean particle size for the 1st break with decreasing moisture content, which was validated by lab scale milling trials.

Even though the model could accurately predict the trend with changing moisture content, the percent deviation of prediction was high. The reason for the high deviation could be attributed to the following: the use of uniformly sized particles to represent the 1st break; and the uniform bond strength used to bond the cluster. For the purpose of creating the bonded cluster, uniformly sized spherical particles equivalent to the mean particle size of 1st break were used. However in reality, 1st break is a composition of a wide distribution of particle size including extremely small flour particles with large intact bran particles. In addition, wheat kernel does not have uniform structural strength across its layers. So, the use of uniform bonding resulted in a high relative deviation.

6.3.2.2 Multi-Sphere Approach

The DEM model of 1st break milling operation was also simulated using a multi-sphere approach. In this case, a multi-layered particle resembling a wheat kernel was used to simulate the milling process by assigning a random distribution of bond strength across the kernel. The model predicted a mean particle size of 413 µm for HRW wheat milled at 16% moisture content with a percent deviation of 186 and 157% for lab scale and pilot scale validation, respectively. Similar to the single sphere model, the multi-sphere model accurately predicted the trend in mean particle size when milling wheat at different moisture contents that was validated by lab scale milling trials.

The particle-bond system making up the cluster was given a bond strength distribution within a definite range. However, the model randomly assigned this bond strength value to the particle-bond system of the clusters in a way that it was evenly distributed throughout the cluster which did not exactly replicate the wheat kernel in behavior and resulted in breakage of the cluster into its individual particles ranging in size from 47 µm to 1347 µm. Although the cluster comprised of particles within broad size range, majority these particles had a diameter within 132 µm to 869 µm, which led to the high deviation in model prediction.

6.4 Future Work

Different physical and mechanical properties of wheat kernels, $1^{st}/2^{nd}$ break and wheat flour were measured for three different wheat classes at different moisture levels. The measured properties of wheat were used as inputs for the development of a DEM model of the 1^{st} break wheat milling operation. The model predicted the change in milling behavior of wheat in terms of the particle size and size distribution with changing moisture content. Even though the percent deviation of prediction for the model was high, this study can be applied to understand the 1^{st} break wheat milling operation.

Some future research that could improve the model prediction are:

- Improve model predictability by giving a distributed bond strength replicating the wheat kernel in terms of its components, endosperm, bran layers and germ. Improving model predictability to an acceptable level would enable in accurately simulating the 1^{st} break milling of wheat with varying hardness and moisture levels.
- Using a multi-layered multi-sphere approach in the particle replacement factory during particle cluster formation to simulate a wheat kernel. This could help assemble particles, within the wheat kernel, relating to the inherent chemical composition variation and its relation to hardness and/or strength.

Some of the future practical applications of this study, upon optimization include:

- Developing an understanding on the effect of moisture content and grain hardness on the 1^{st} break milling operation, and the 1^{st} break roll parameters. This could

lead to a greater milling process efficiency and better in-line process control for the milling industry.

- Quantify the force of detachment or the force required to separate the bran layers from the endosperm.
- Capability to compare and understand the difference in 1st break milling behavior of wheat from different classes with varying physical, chemical and mechanical characteristics.